FINAL REPORT
Improving attachments of remotely-deployed dorsal fin-mounted tags: tissue structure, hydrodynamics, in situ performance, and tagged-animal follow-up

Russel D. Andrews
University of Alaska Fairbanks and the Alaska SeaLife Center
P.O. Box 1329, Seward, AK 99664
phone: (907) 224-6344 fax: (907) 224-6371 email: russa@alaskasealife.edu

Robin W. Baird and Gregory S. Schorr
Cascadia Research Collective
218 ½ W 4th Ave., Olympia, WA 98501
phone: (360) 943-7325 email: rwbaird@cascadiaresearch.org gschorr@cascadiaresearch.org

Rajat Mittal
Cartesian Flow Solutions, Inc.
Vienna, VA 22181
Phone: (703) 242-6602 email: mittalr@gmail.com

Laurens E. Howle
BelleQuant Engineering
Mebane, NC
phone: (919) 210-3056 email: leh@bellequant.com

M. Bradley Hanson
NOAA Northwest Fisheries Science Center
2725 Montlake Boulevard East, Seattle, WA
phone: (206) 860-3200 email: brad.hanson@noaa.gov

Grant Number: N000141010686
http://www.alaskasealife.org

Grant to Collaborating Federal Entity: N0001412IP20008 (PI: Hanson)
http://www.nwfsc.noaa.gov/research/divisions/cbd/marine_mammal/marinemammal.cfm
Date of Report: 31Mar2015

LONG-TERM GOALS

We recently developed small satellite-linked telemetry tags that are anchored with small attachment darts to the dorsal fins of small- and medium-sized cetaceans. These Low Impact Minimally-Percutaneous External-electronics Transmitter (LIMPET) tags have opened up the potential to monitor the movements of numerous species not previously accessible because they were too large or difficult to capture safely, but too small for tags that implant deeply within the body. In this project we aim to improve upon our existing tagging methodology to achieve longer, less variable attachment durations by carefully examining the factors that affect attachment success. Our key goal is to develop a method for attaching tags to cetaceans that provides the data needed to answer critical conservation and

management questions without an adverse effect on the tagged animal. Therefore, our project includes follow-up studies of whales that have been tagged with a remotely-deployed dorsal fin-mounted tag to accurately quantify wound healing and the effects of tagging on whale survival, reproduction, and behavior. The combination of these approaches should provide an improved understanding of some of the key factors affecting tag attachment duration as well as a more complete understanding of impacts to individuals due to tagging.

OBJECTIVES

1. Design an improved barnacle-style tag shape for remote-deployment by assessing the hydrodynamic properties of tag shapes
2. Examine the tissue structure of the dorsal fin and its material properties for better informed implanted attachment design.
3. Examine the in situ performance of our current attachment devices and then design and test improved retention systems
4. Conduct follow-up studies of tagged whales to quantify wound healing and the effects of tagging on whale survival, reproduction, and behavior

APPROACH

1. Hydrodynamics of tag shape (Key individuals: Mittal, Howle, Andrews, Schorr, Hanson): We will determine the hydrodynamic forces acting on the tag through numerical modeling and analysis, primarily computational fluid dynamics. High fidelity numerical simulations working in concert with physical experiments in a water tunnel will be used to establish qualitative as well as quantitative relationships between tag configuration and the associated flow structure and surface pressure distribution, which is ultimately the key to the forces/moments on the tag.

2. Dorsal fin tissue structure (Key individuals: Hanson): To evaluate the factors influencing tissue degradation (and therefore attachment duration) we will assess the anatomical factors likely to influence long-term viability. Interspecific differences in these parameters may be an important factor in the variability in attachment duration, as might body size scaling effects. We selected various species for examination based on differences such as size/shape of the dorsal fin (e.g., pygmy killer whale versus killer whale), taxonomic grouping (i.e., odontocetes versus mysticetes), or dynamic behavior (*e.g.*, beaked whale versus false killer whale).

3. Performance of tag attachments – simulated and actual (Key individuals: Andrews, Schorr, Hanson, Howle, Mittal): A key factor in attachment duration is likely the hydrodynamic forces imposed by the tag body but acting on the attachment elements implanted into the dorsal fin. Although we have a good idea of how the LIMPET retention system operates when first implanted, we do not fully understand the mechanics in a living fin. Therefore, we will use non-invasive imaging of carcass tissue to determine how the retention elements behave in situ. These results, along with those from the analysis of dorsal fin histology and material properties will inform modified designs. Hundreds of LIMPET tags have now been applied to various species of cetaceans, and we will examine inter-species differences and explore factors that effect tag longevity.

4. Tagging effects - follow-up studies of survival, reproduction,& behavior (Key individuals: Baird, Schorr, Andrews, Hanson): More thorough assessments of the potential impacts on survival and reproduction of individuals, as well as assessment of healing of the tag attachment sites and potential behavioral changes associated with tagging, are needed to address concerns regarding sub-lethal and potentially lethal impacts of remotely-deployed tags. As part of an ongoing collaborative study, many hundreds of satellite and VHF tags have been remotely-deployed on 10 species of odontocetes around the main Hawaiian Islands. Re-sighting rates for the two species with the largest sample size of tag deployments, short-finned pilot whales and insular false killer whales, are particularly high, as populations are small, individuals are relatively easy to approach, and there are sufficient encounters each year to have a high probability of re-sighting previously tagged whales. We will assess impacts of remotely-deployed tags on tagged animals at a variety of levels: from wound healing and potential behavioral effects of tag attachment to reproduction and survival. Assessment of reproduction and survival of tagged whales will utilize existing photographic datasets as well as additional photos taken during this project.

Objective 1: Hydrodynamics of tag shape

WORK COMPLETED

At the start of the this project, the standard location-only SPOT5 LIMPET tag was Wildlife Computers model AM-240B (Fig. 1, left). At that time, over 200 deployments of this tag and its very similar predecessor the AM-240A had occurred, and although most deployments went very well, in a few instances the force of impact on off-angle shots resulted in the cracking of the epoxy where the dart inserts into the tag (Fig. 2). To address cracking of the tag epoxy, we worked with Wildlife Computers to design and produce a tag that should be much less susceptible to cracking upon impact (new model: AM-240C, Fig. 1, right). The electronics are first cast into a rigid epoxy, and then the tag is over-molded with a very strong urethane that contains the threaded dart holes. The design of this tag was based upon preliminary hydrodynamics work conducted under this project. The shape is a compromise between the challenges we face from aerodynamic issues during remote deployment and the hydrodynamic issues once the tag is attached to the whale. Dimples and bumps were added to create turbulence in order to delay flow separation in the hopes of reducing the drag on the tag. The placement of the dart attachment holes also changed – in the 240C tag a line connecting the two dart thread holes is perpendicular to the long axis of the tag body instead of running along it. This brings the two darts closer together, reducing the impact stress during off-angle shots. Below we compare the hydrodynamic properties of these two designs under varying conditions using both computer simulations and tests with physical models in a water tunnel.

Work in computational fluid dynamics (CFD) modeling focused on understanding the effect of tag design as well as tag orientation and location on hydrodynamic forces. Initial work focused on drag but our hypothesis was that lift forces might also play an important role in tag detachment. A sequence of 3D, unsteady direct numerical simulations were carried out for two different tag designs (old AM-240B and new AM-240C) The simulations employed an immersed boundary solver that allowed us to simulate flow past complex boundaries on fixed Cartesian grids (Mittal et al. 2008). The simulations, being 3D and unsteady, required super-computing resources and we employed large-scale parallel computers for these simulations. Given that the typical sequence of tag migration and eventual detachment involves an increase in the gap between the tag and the epidermal surface as well as an upward tilting of the leading edge of the tag, we have used CFD simulations to examine the effect of both these features on the hydrodynamic forces. Figure 3 illustrates the overall model of the forces acting on the tag and how these forces produce a pulling (detachment) force on the tag. We

characterized both the force of lift and drag on the tag and the effect of gap size, angle-of-attack (AOA) and orientation, or angle of rotation (ROT), on these forces (Fig 4a, b).

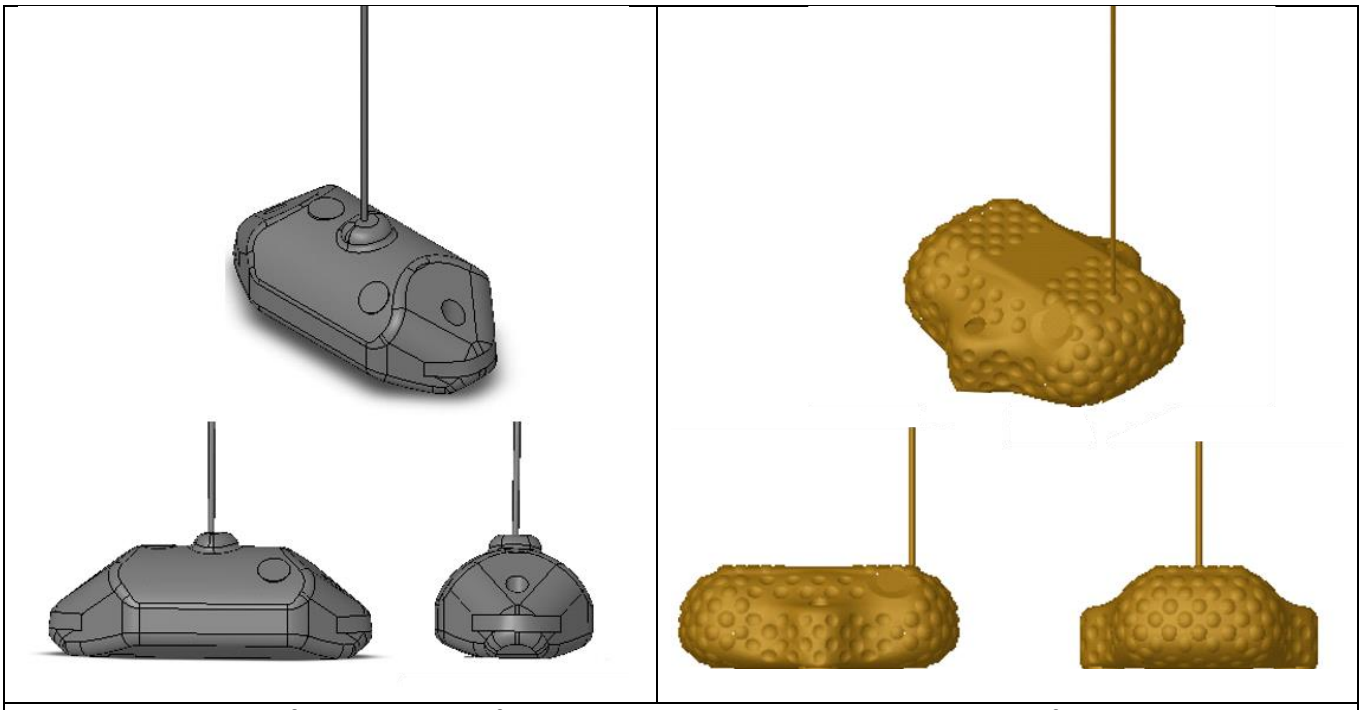

Fig. 1. Illustrations of two versions of the LIMPET SPOT5 tag without darts. Left, old AM-240B; Right, new AM-240C.

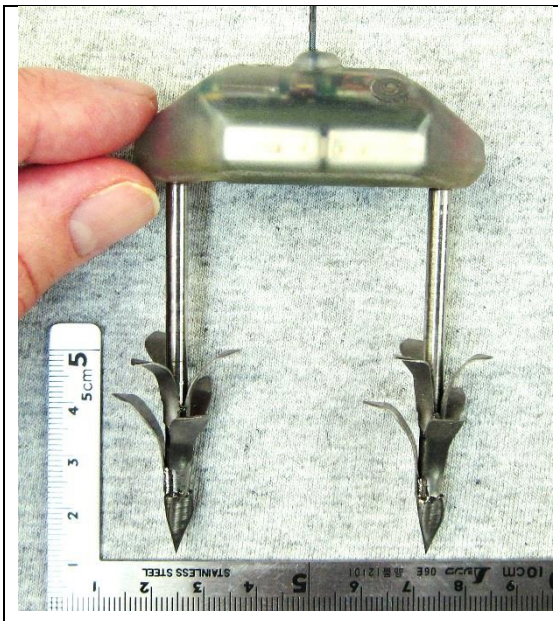

Fig. 2. Photo of AM-240B – fingers are gripping epoxy where it could potentially break upon impact.

In preparation for water tunnel tests with physical models, a separate set of CFD simulations were run using the SolidWorks Flow Simulation package. Although this software provides much lower resolution than is possible with the immersed boundary solver method, the computation time is drastically reduced. The simulations were run using incompressible flow conditions and used a RANS turbulence model for flow speeds ranging from 1.0 to 10.0 ms^{-1} and orientations ranging from 0 to 90 degrees. The sign convention used in reporting the forces is shown in Figure 5. In the results section presented below, the forces and flow speeds were corrected from model scale and experimental conditions to actual scale and seawater conditions using standard similitude techniques.

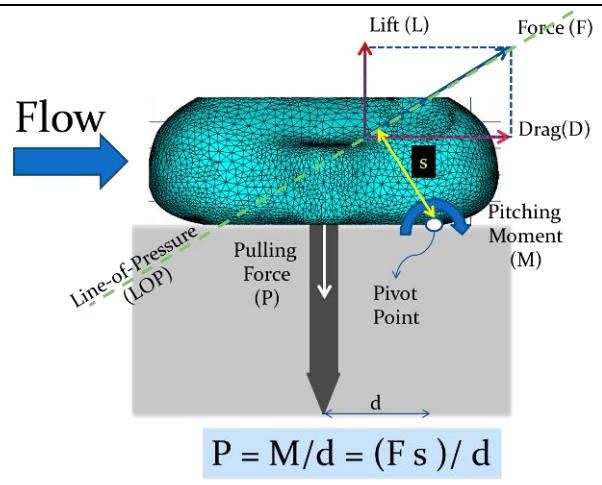

Fig. 3. Schematic illustrating the various forces and moments acting on the AM-240C tag. Note that the pulling force `P` is proportional to the pitching moment `M`.

Computational Fluid Dynamics studies were also undertaken in the SolidWorks Flow Simulation CFD package to compare the most recent iterations of the LIMPET tag designs, the location-only AM-240C tag and the dive depth-transmitting AM-292 tag. The studies included a flow speed sweep at a fixed orientation, a yaw angle study (tag rotated about a vector normal to the mounting surface), a inclination angle study (tag rotated about a vector that was the cross product of the free-stream flow direction and the mounting surface normal vector), an offset study (offset = distance from the bottom of the tag and the dorsal fin or surrogate mounting surface), and a study combining inclination and yaw. CAD models of the two tag types, in SolidWorks format (Fig. 6), were provided by Shawn Wilton of Wildlife Computers and were imported directly into the SolidWorks Flow Simulation package.

Water tunnel experiments with physical models of the tags were made in the closed-circuit water tunnel at the United States Naval Academy using the Bellequant Engineering force measurement system. Measurements of lift, drag, and side forces were made with submersible Hydronautics force transducers and the angle of the model was measured by a multi-turn potentiometer mounted on a custom built quadrant (Weber et. al., 2009, 2010) as shown in Figure 7. The tunnel employed turning vanes in the corners and a honeycomb flow straightener in the settling chamber. Free-stream turbulence was found to be ~0.5% (Schultz and Flack, 2003). Two configurations of the AM-S240C tag were tested, one with a smooth outer surface and one with a combination of convex and concave dimples to determine the drag-reducing effect of dimples, and these were compared with the old AM-240A tag. The three tag models at 2:1 scale were constructed from ABS plastic using fused deposition modeling (FDM). The three tag configurations tested were the new AM-240C tag with a smooth

surface finish (SmoothTag), the AM-240C tag with surface dimples and bumps (Dimpled Tag), and the AM-240A tag with a smooth surface finish (Old Tag). This rapid prototyping (RP) process produces slightly rough surfaces with a layer thickness of 0.254 mm. Before testing, each of the three tags was coated with several layers of Marine primer and sanded fair. This process eliminated the irregularities caused by the fused deposition modeling process. The dimpled tag was carefully finished so that the bumps remained intact but the FDM irregularities were filled and faired. Models were evaluated at flow speeds ranging from 1 m/s to 5.5 m/s, and orientations (Angle or Rotation) ranging from -20 to +90 degrees (with the zero angle indicating tag alignment with the flow). These flow speeds corresponded to Reynolds numbers in the range of 56,000 to 310,000.

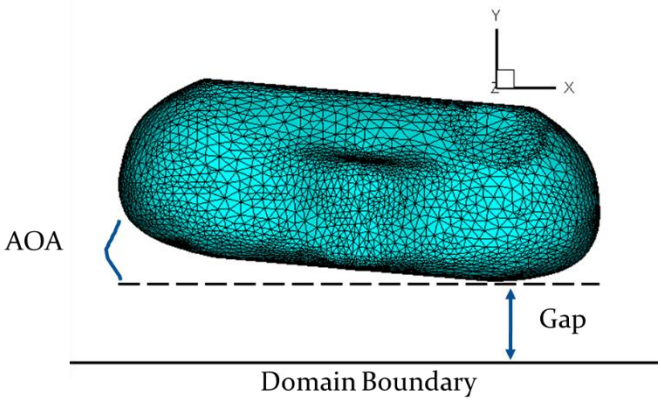

Fig. 4a: Illustration of Angle of Attack (AOA) and Gap, the distance between bottom of tag and attachment surface (computer simulated boundary or whale skin)

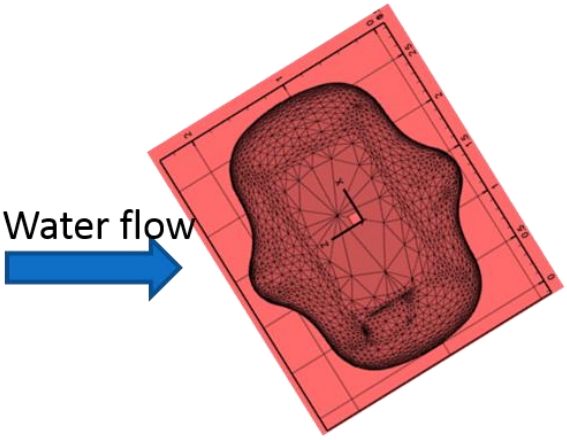

Fig. 4b: Illustration of Angle of Rotation (ROT) with tag rotated 45 degrees relative to the direction of water flow.

Fig. 5. Computer model of old model AM-240A (left) and force sign convention used for reporting the results (right). Flow is from left to right. The blue, red, and green arrows indicate, respectively, positive lift, drag, and side forces. The clear arrow indicates positive rotation angle.

Fig. 6. CAD models of the most recent designs of the location-only LIMPET tag (AM-240C, Left) and the dive depth-transmitting LIMPET tag (AM-292, Right). The antennae and wet-dry sensors were removed to simplify the computational mesh.

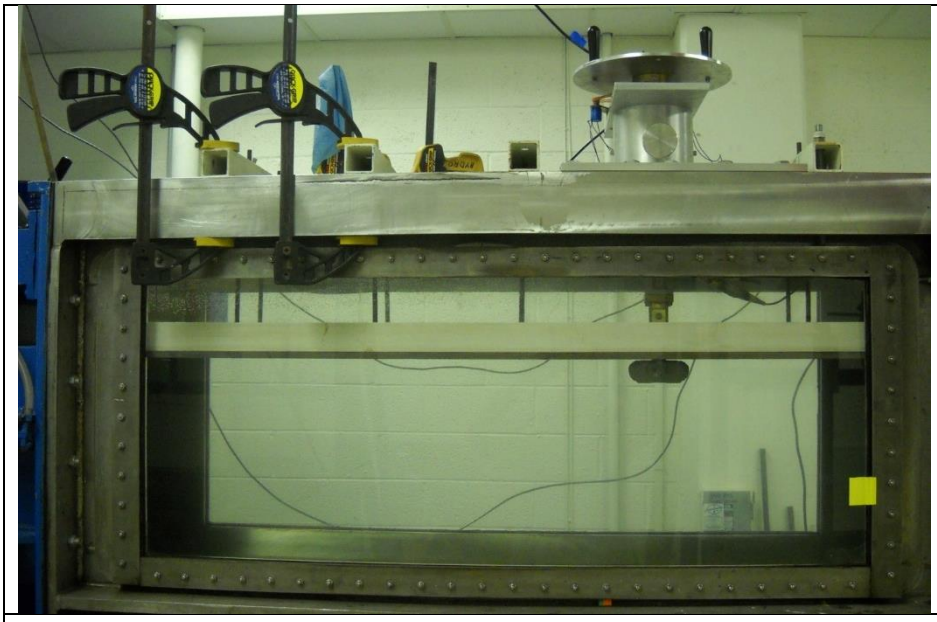

Fig. 7. AM-S240C tag mounted in the US Naval Academy water tunnel test section.

Objective 1:

RESULTS

Figure 8 shows the computed vortex structures for the new tag (AM-240C) with zero gap and zero inclination. The flow over the tag and in the wake of the tag is highly three-dimensional and consists of a number of distinct vortex structures. The wake also exhibits vortex shedding. These features are typical for all the tag configurations studied. Figure 9 shows the effect of gap on the drag (Fx) and lift (Fy) forces on the tag. The drag force on the tag is relatively independent of the gap whereas in contrast, the lift force depends significantly on the gap. The lift force is highest for zero gap and decreases monotonically to a low value as the gap increases. The highest value of lift for the zero gap is comparable to the value of drag. This implies that in its initial stages of attachment when the tag is

snug with the epidermal surface, both lift and drag forces are important whereas with increasing gap (and zero inclination, AOA), drag becomes the dominant force on the tag. Figure 10 shows the effect of angle of attack on the hydrodynamic forces experienced by the tag. For the case with zero gap, a positive inclination of 5 degrees increases both the lift and drag. However, while the increase in drag is small (~ 15%), the increase in lift is very large (~ 50%). This leads to a situation where the lift is roughly twice the value of drag. A similar behavior is observed for a case with a finite gap (gap = ¼ the tag height); drag forces show marginal increase whereas lift forces increase by over 100% with a small inclination. Based on all of the above simulations, it is clear that the most unfavorable situation for the tag is when the gap is small and the inclination is large.

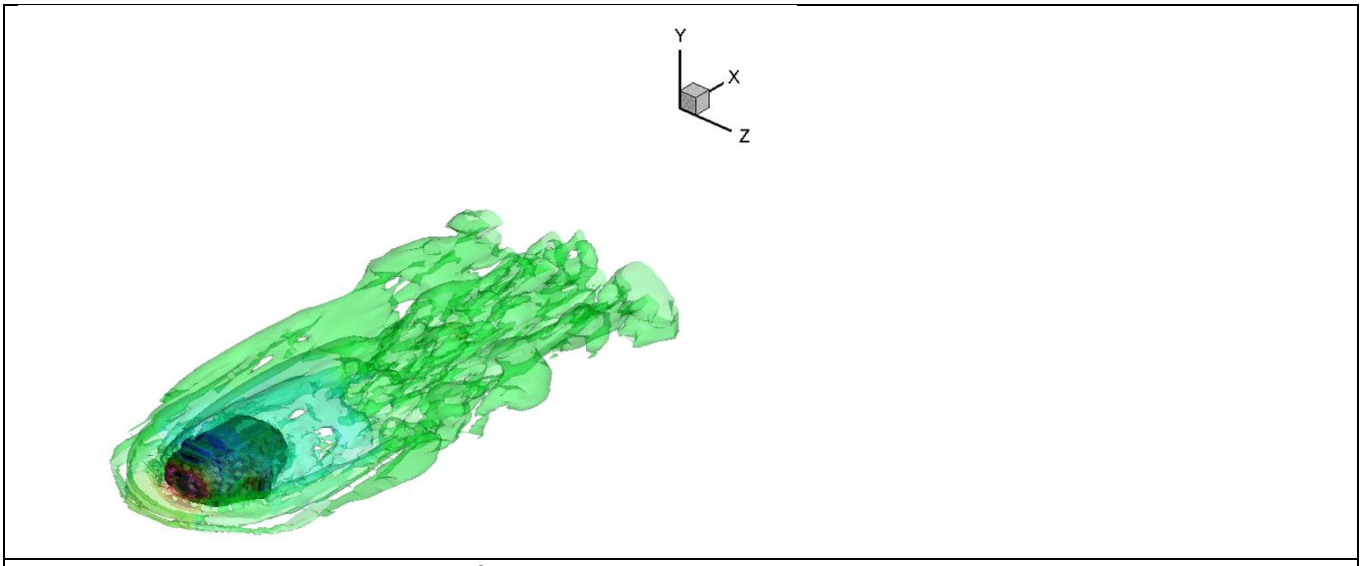

Fig. 8. Vortex structures computed for the new tag (AM-240C) with zero gap and zero inclination.

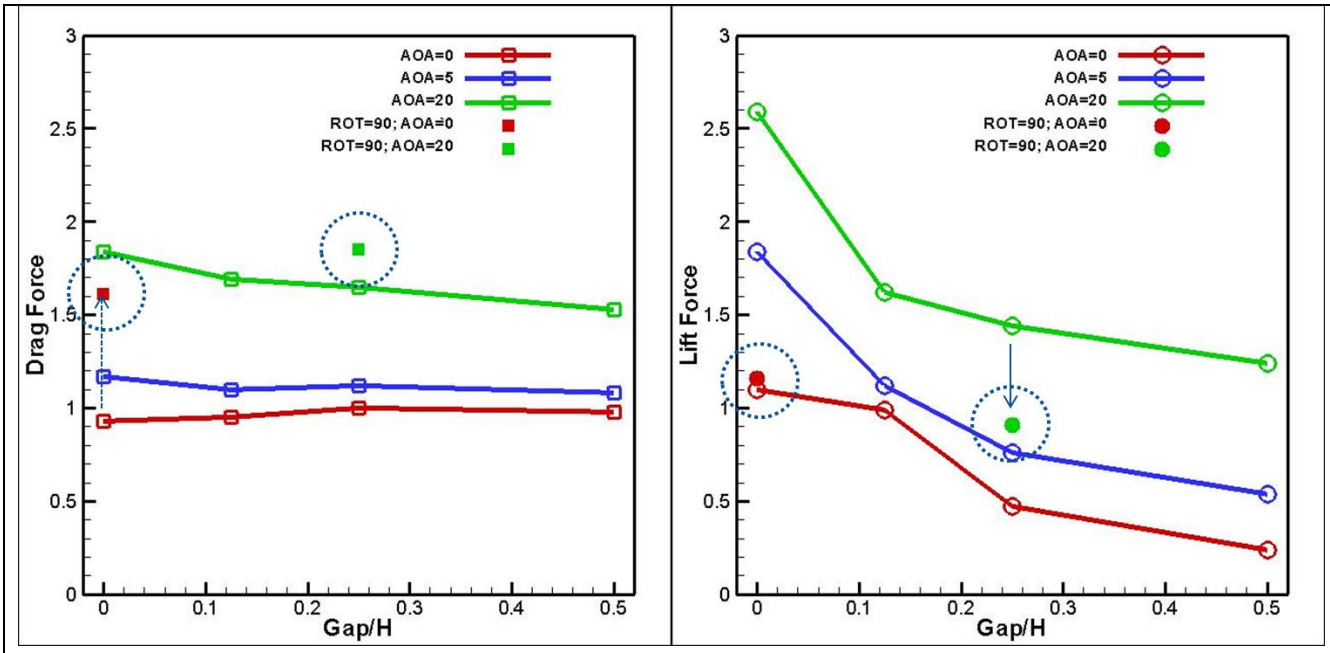

Fig. 9. CFD results showing how drag (Fx) and lift (Fy) forces on the tag vary with the size of the gap as well as angle-of-attack (AOA) and orientation (ROT).

Finally, the change in orientation of the tag in relation to incoming flow has a more complex effect on both forces with the drag force showing increase and the lift force showing no change or a decrease based on the initial angle-of-attack. Based on our simple model of the tag forces (see Fig. 3), the hydrodynamic pulling force on the tag is proportional to pitching moment. Thus Figure 10b shows that the net pulling force is highest for small gaps and large inclination angles and that in this condition, lift is the dominant contributor to the pulling force. For large gaps, the pulling force is reduced and drag is the primary contributor to the pulling force.

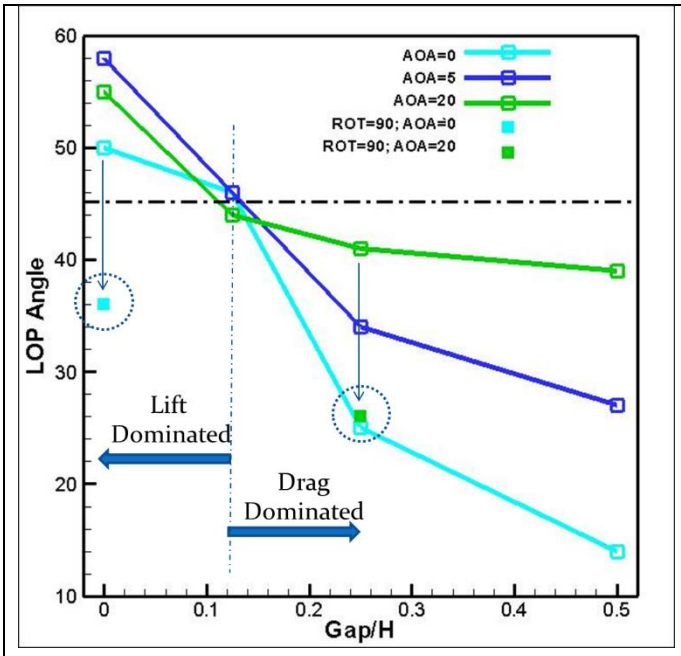

Fig. 10a. Effect of gap, angle of attack (AOA) and orientation (ROT) on the direction of the net force

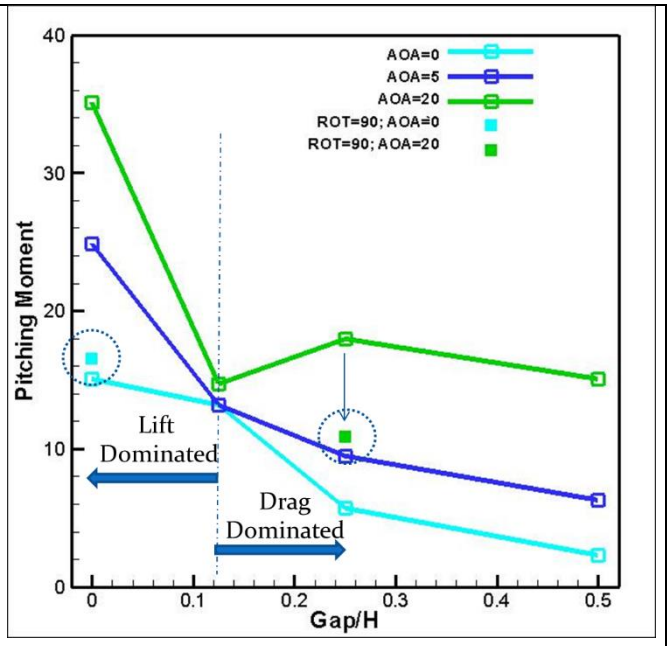

Fig. 10b. Effect of gap, AOA and ROT on the pitch up moment on the tag.

The Solidworks CFD results showed recirculation on the downstream side of the tag. This recirculation was found to result in unsteady vortex shedding (Fig. 11) for some flow speeds and orientations. The CFD-generated predictions of drag displayed typical quadratic dependence on flow speed. These CFD results were used to select the force transducers for our water tunnel study.

Water tunnel testing results include a comparison of the scaled drag force (Newtons) versus the scaled flow speed (m/s), as shown in Figure 12, indicating that there is little difference in drag between the three tag designs. However this only holds when the tag is aligned with the flow, with its long axis parallel to the flow direction. As Figure 13 shows, the old tag (AM-240A) produces substantially more drag (up to 2X) for flow angle orientations greater than ±30°. In Figures 13 - 15 , the scaled flow speed is held constant at 5 m/s. The comparison of the side forces versus flow orientation produced by the three tags, shown in Figure 14, shows that the old tag produces substantially greater side force for flow orientations between 20° and 70°. At the extreme, the old tag produces approximately 3X the absolute side force. The lift force versus rotation angle for the three tags is shown in Figure 15. In contrast to the drag and side forces, the old tag produces lower lift over the entire range of flow orientations.

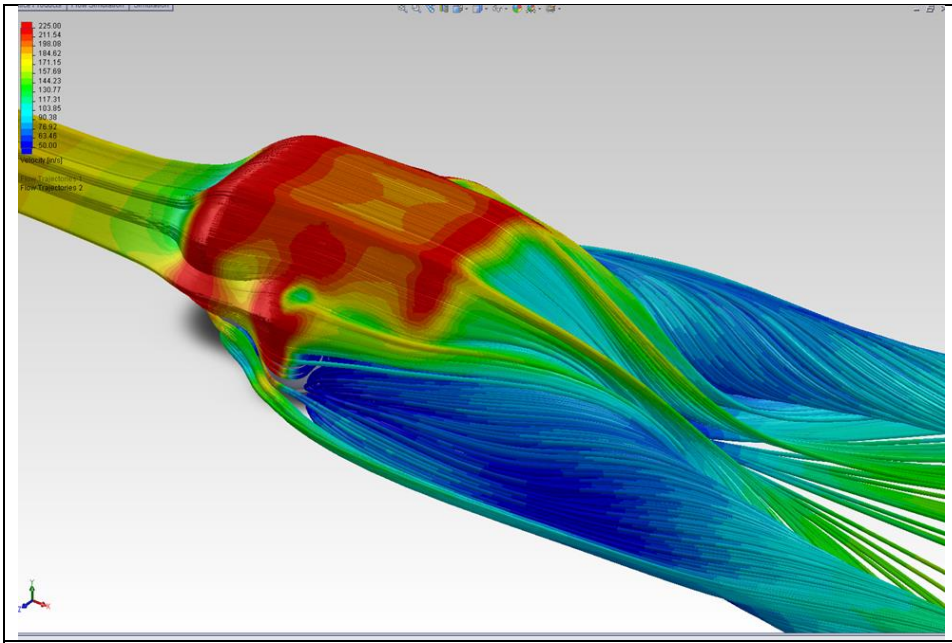

Fig. 11. Particle path lines for flow past the AM-S240C tag. In this SolidWorks CFD simulation, water flows from upper left to lower right. Notice the counter-rotating vortex pairs on the downstream end of the tag indicating lifting flow.

Based on our water tunnel measurements we can make the following conclusions concerning the three tag designs. (1) The old tag (AM-240A) generates lower lift than the new tag in either the Smooth configuration or the Dimpled configuration across all flow orientations and flow speeds. (2) At lower flow orientation angles, the Old Tag produces lower drag and side forces than either the Smooth Tag or the Dimpled Tag across all flow speeds. (3) Above approximately 20° the Old Tag generates substantially more drag (up to 2X) and side force (up to 3X) compared to either the Smooth Tag or the Dimpled Tag. (4) Surface bumps on the dimpled tag (compared to the smooth tag), offer no clear advantage other than to flatten out the lift dependence on the flow orientation angle but this only holds at higher flow speeds. Given that we currently cannot control the rotation of the tag in flight, it appears that the new Dimpled tag has a slight advantage with the lowest overall (drag plus lift) pulling force at a variety of rotation angles.

Flow speed study: CFD simulations were conducted at flow speeds of 0.75, 1.50, 3.00, 5.00, and 7.00 m/s. For this flow speed study, the tags were aligned with the oncoming flow (yaw angle = 0 degrees, pitch angle = 0 degrees). In Figure 16, drag force is graphed as a function of flow speed, demonstrating the characteristic quadratic dependence of drag with flow speed. Note that the AM-292 tag has slightly greater drag over the range of flow speeds considered. The lift force, similar to the drag force was slightly greater for the AM-292 tag than for the AM-240C tag (Fig. 16).

Yaw angle study: We define the yaw angle as a rotation about the mounting surface normal vector. CFD simulations were performed for yaw angles of 0, 45, and 90 degrees at a fixed flow speed of 1.5 m/s. Both tags showed an increase in drag (Fig. 17, left) with yaw angle. This is consistent with expectations as the 90 degree yaw orientation presents a greater projected area to the oncoming flow. The lift force (Fig. 18, right), first increases and then decreases with yaw angle.

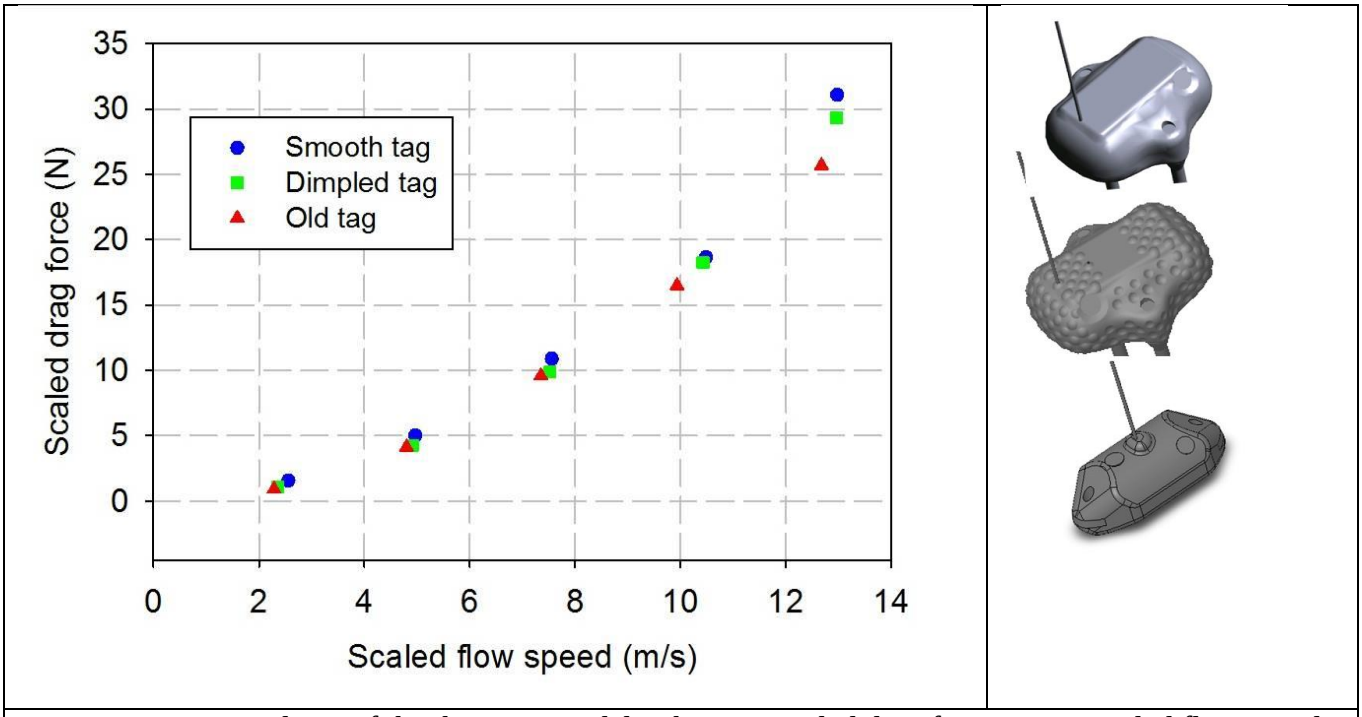

Fig. 12. Water tunnel test of the three tag models, showing scaled drag force versus scaled flow speed for the tag with its long axis parallel to the direction of flow (0° rotation, ROT). Note that there is little difference between tag types in the scaled drag force over this range of flow speeds.

Inclination angle study: The inclination angle (Fig. 18) was defined as positive when the leading edge lifted away from the mounting surface. For this study, the flow speed was held constant at 1.5 m/s and the yaw angle was fixed at 0 degrees. Increasing the inclination angle increases the drag force (Fig. 18, left). This approximately 2.5x increase over the inclination angle range of 0 to 40 degrees results from increased projected frontal area with increased inclination angle. In contrast to the drag force, the lift force (Fig. 18, right) did not show a monotonic trend over this same range of inclination angles for both tags. The AM-292 tag generated increased lift for 0 and 20 degree inclination angles whereas the AM-240C tag generated increased lift at 40 degrees.

Offset study: An offset study was performed at two offset heights, 0.01in and 0.25in. Offset was defined as the gap between the mounting surface and the lower surface of the tag housing. Both tags showed similar results when gap increased from 0.01in to 0.25in. For both tags, the lift force dropped off while the drag force showed little change. The AM-24C tag had a lift force of 0.6915N at 0.01" offset, but dropped by 72%, to 0.1942N, at 0.25" offset. The lift force dropped by 59% with the increase in offset, from 0.8413N to 0.3415N.

The CFD comparison of the AM-240C and AM-292 tags indicated that the AM-292 tag generated somewhat higher lift but primarily at flow speeds above 5 m/s and aligned flow (0° yaw angle). The AM-292 tag also generated somewhat higher drag than the AM-240C tag. At a fixed flow speed of 1.5 m/s both tags showed a fairly weak dependence of lift and drag on yaw angle. Both tags demonstrated an increase in drag of approximately 2.5x for inclination angles up to 40°. As shown in our previous studies, an increase in gap (offset) from almost touching the mounting surface to about 0.3 times the height of the tag, caused a shift from lift-dominated to drag-dominated force. Overall, the AM-240C

tag produced somewhat lower lift and drag than the AM-292 tag for most of the flow scenarios considered.

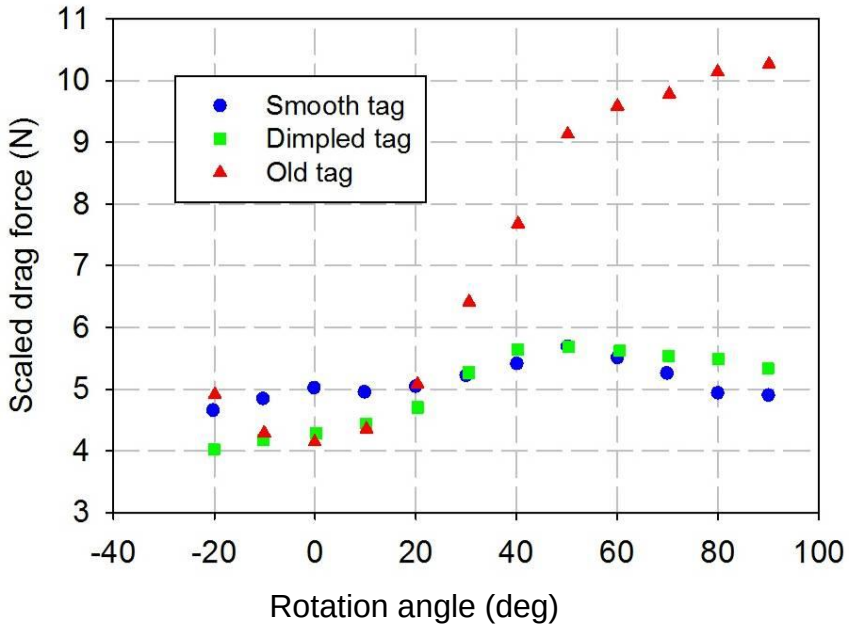

Fig. 13. Water tunnel results comparing the scaled drag force versus rotation for the three tags considered in this study at a flow speed of 5 m/s. Note that at flow orientations greater than ±30°, the old tag produces considerably greater drag.

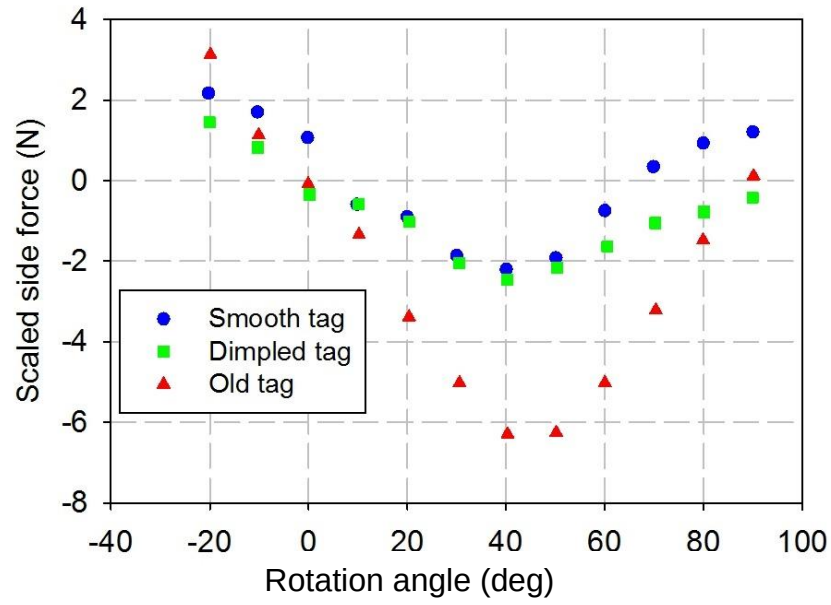

Fig. 14. Water tunnel results comparing scaled side force versus rotation angle at a fixed scaled flow speed of 5 m/s. The old tag produces substantially greater side force than either the smooth tag or dimpled tag for orientations in the range of 20° to 70°.

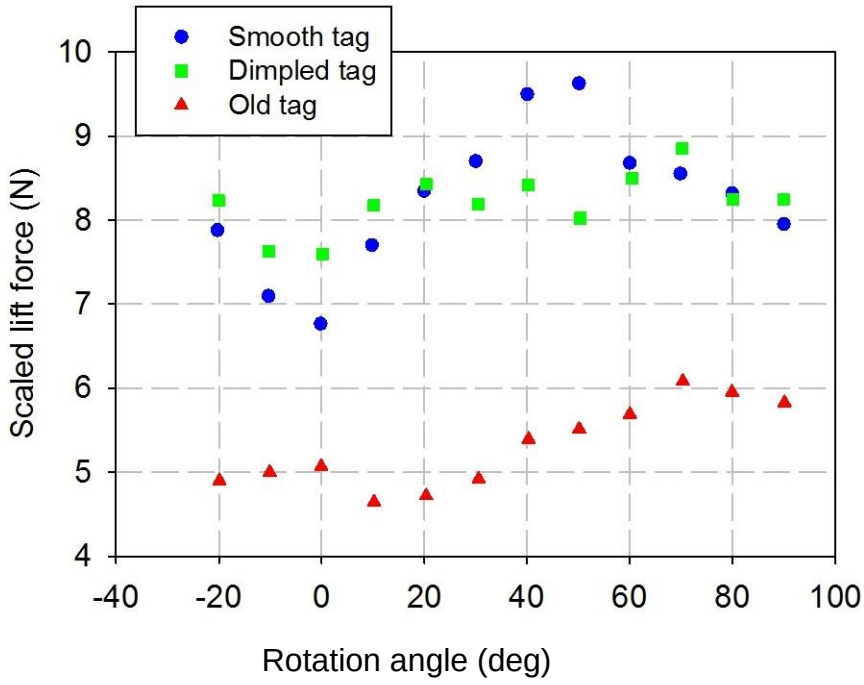

Fig. 15. Water tunnel results comparing scaled lift force versus rotation angle for the smooth, dimpled, and old tags at a constant flow speed of 5 m/s. The lift force is lower for the old tag over the entire range of flow orientations.

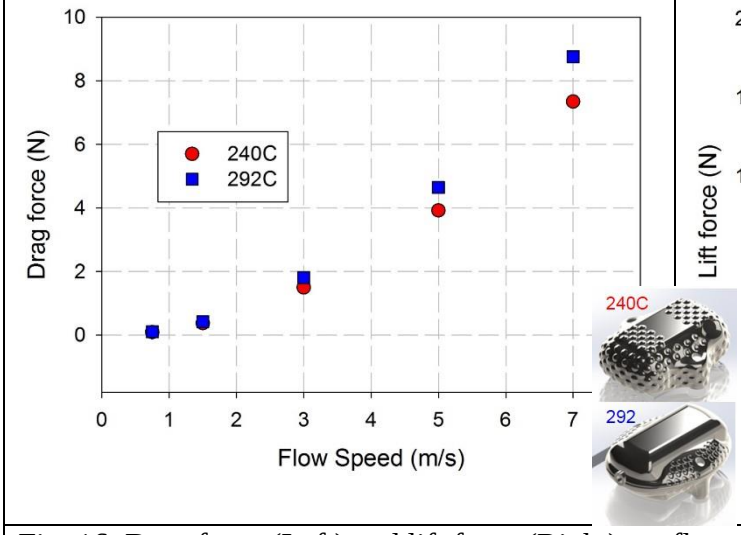

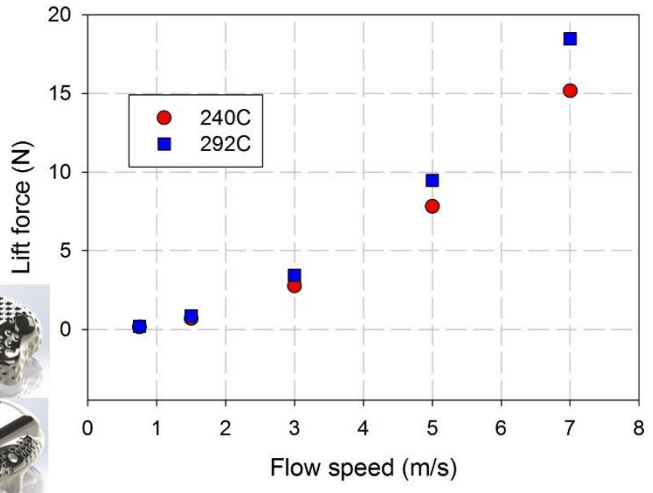

Fig. 16. Drag force (Left) and lift force (Right) vs. flow speed at 0 degree yaw and pitch angles for the AM-240C and AM-292 tags. The AM-292 tag generated slightly more drag and lift than the AM-240C tag, but it was only significant at higher speeds.

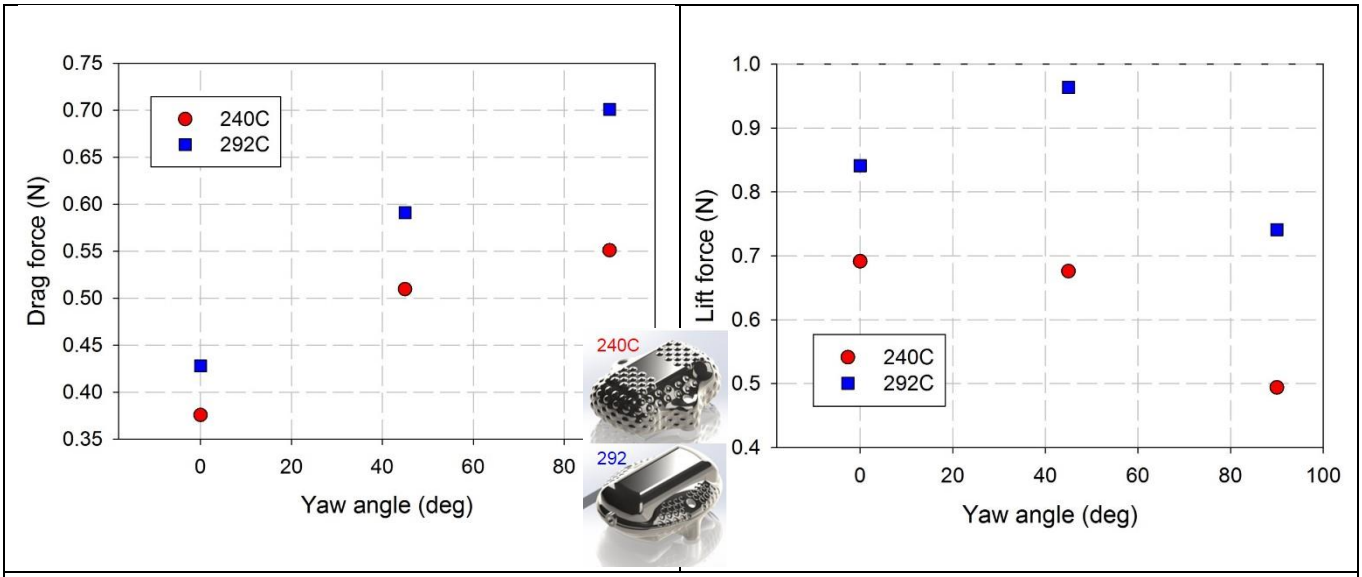

Fig. 17. Drag force (Left) and lift force (Right) at different yaw angles (=angle of rotation, ROT), at a fixed flow speed of 1.5 m/s, for the AM-240C and AM-292 tags.

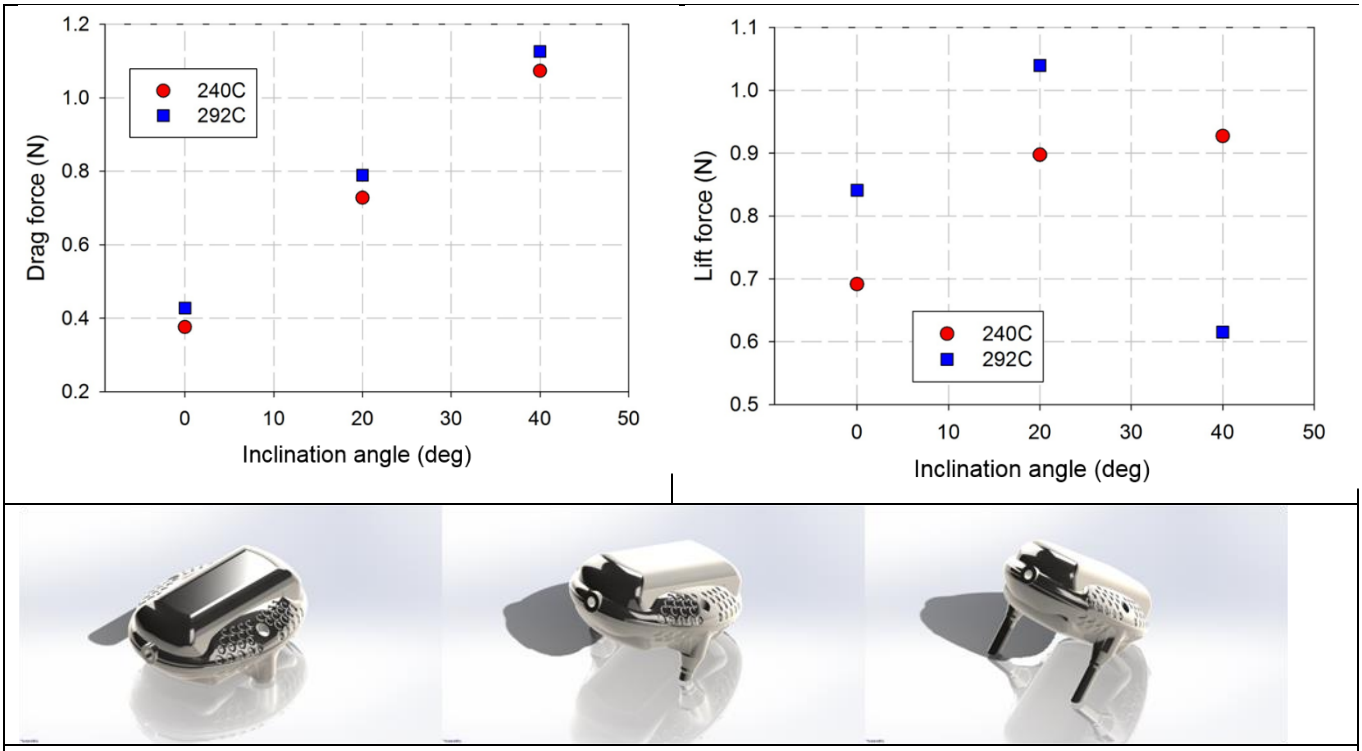

Fig. 18. Top: Drag force (Left) and lift force (Right) at various inclination angles. Bottom: inclination angles of 0° (left), 20° (center), and 40° (right). Flow direction: lower left to upper right.

Objective #2: Dorsal fin tissue structure

WORK COMPLETED

Dorsal fins were collected from beach-cast specimens of eight species of cetaceans – harbor porpoise, pilot whale, killer whale, false killer whale, pygmy killer whale, Bryde's whale, Cuvier's beaked whale, and Blainville's beaked whale. We used these dorsal fins to assess the geometry and collagen composition of primary structural layers, and to determine the stress/strain characteristics of the load-

bearing tissues (the ligamentous sheath and the central core). In addition to examining differences between species, we used the killer whale fin to examine the potential variation in collagen composition and material properties at various locations of the fin.

Frozen dorsal fins were thawed and an approximately full depth section of fin tissue, approximately 3mm high by 25 mm in width, was removed from approximately mid-fin (in both the dorsal-ventral and anterior-posterior axes) of each fin and fixed in formalin for histological analysis of the tissue layers. Adjacent sections were also removed to measure the material properties of the two primary collagen-bearing layers of the dorsal fin (ligamentous sheath and central core) for these 8 species using an uniaxial tester to build stress/strain curves. In order to assess the strength of the tissue of the eight cetacean species, and five areas of the killer whale fin, the yield point was estimated by fitting a hierarchical Bayesian Gompertz growth model to the stress-strain tissue data. The model was separately applied to two datasets: the ligamentous sheath data, and central core data, for the eight cetacean pieces and the five areas of the killer whale fin.

Objective 2:

RESULTS

Dorsal fin structure

The thickness of the epidermis, subpapillary layer, and ligamentous sheath combined was greatest in the killer whale, nearly twice the overall thickness of the next closest species, the pilot whale, and the thinnest was the Blainville's beaked whale (Table 1). Similarly, the killer whale (mid-fin area) also had the thickest ligamentous sheath, but the pygmy killer whale had the second thickest and harbor porpoise the thinnest. The subpapillary layer thicknesses followed the same trend as the total thickness. Interestingly, the epidermis/dermal papillae layer was 2-3 times thicker in the harbor porpoise than the other species. Comparing the five areas of the killer whale fin, the ventral and the anterior region had a greater combined thickness (epidermis/sub-papillary layer/ligamentous sheath) than the mid-fin area. Much of this increase was associated with the greater thickness of the ligamentous sheath, as well as the epidermis/dermal papillae layer.

Table 1. Lateral thickness (mm) of the dorsal fin tissue layers in the mid-fin area (in the dorsal-ventral and anterior-posterior axes) of different species and in different areas of the killer whale fin.

Species	Epidermis/ dermal papillae	Sub-papillary layer	Ligamentous sheath	Total thickness
Harbor porpoise	3.2	0.1	1.1	4.3
Pygmy killer whale	1.2	1.4	3.6	6.2
Brydes whale	1.6	2.2	2.9	6.7
Cuvier's beaked whale	1.1	2.1	2.2	5.4
Pilot whale	1.7	2.8	3.2	7.7
Blainville's beaked whale	0.9	0.9	1.8	3.6
False killer whale	0.6	1.3	2.8	4.7
Killer whale (Dorsal)	2.0	3.1	2.8	7.9
Killer whale (Anterior)	2.4	5.1	7.6	15.1
Killer whale (Central)	1.8	5.2	6.3	13.3
Killer whale (Posterior)	1.0	2.8	3.5	7.3
Killer whale (Ventral)	2.8	4.4	9.8	17.0

Percent collagen in the ligamentous sheath was consistently high in all species, ranging from a high of 96% in the pilot whales to a low of 75% in Blainville's beaked whales (Fig. 19). Inter-species variability was greater for the central core where the pilot whale again had the highest % collagen (81%), and the Blainville's beaked whale was lowest at 42%. For the different areas in the killer whale fin, the mid-fin and anterior areas had the highest % collagen for ligamentous sheath tissue, while for the central core the dorsal and posterior areas were the highest, with their collagen content being very similar to the ligamentous sheath (Fig. 20).

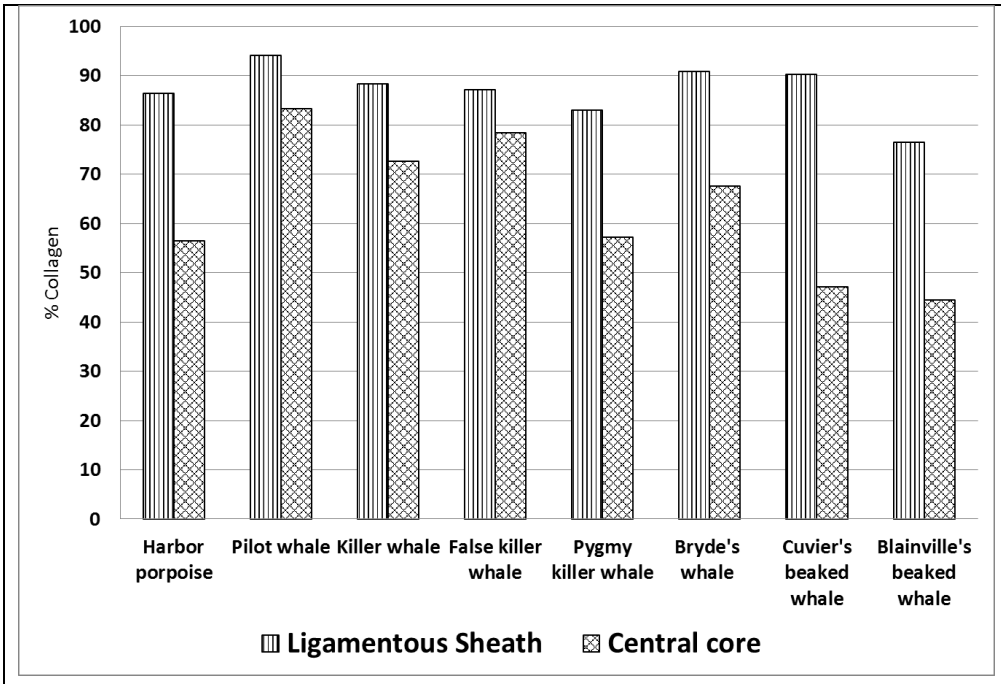

Fig. 19. Percent collagen in the ligamentous sheath and central core of the dorsal fins of eight cetacean species.

Dorsal fin material properties

The stress/strain curves developed for the ligamentous sheath of the eight cetacean species (dorsal-ventral orientation (Fig. 21a) and central core (anterior-posterior orientation; Fig.21b) all exhibited the non-linearity associated with collagen-bearing viscoelastic tissues. The ligamentous sheath generally had steeper slopes than the central core and displayed a greater yield point for a particular strain value than did the central core. The greatest yield point in ligamentous sheath was observed for the false killer whale, with Blainville's beaked, Pygmy killer, and Bryde's whales falling below, and Cuvier's beaked, pilot whale, and harbor porpoise at a somewhat similar level below those species. Killer whale was the lowest, at about half the yield point of the false killer whale. For the central core the slopes in the elastic region for all species were more variable and generally lower than those observed for the ligamentous sheath, as were yield points. High yield points were again observed for Blainville's beaked and Bryde's whales, and although harbor porpoise was the lowest, the killer whale sample was observed to again be relatively low. For the comparison of material properties of the different areas within the killer whale fin, the ligamentous sheath displayed more stiffness than the corresponding areas of the central core in the elastic region of the stress/strain curves (Fig. 22a, b). However, the ligamentous sheath values within the fin exhibited a variety of different slopes with the dorsal area being the stiffest and the posterior area the least stiff. The dorsal area of the ligamentous sheath also

had the greatest yield point while the ventral section had the weakest, with the other areas somewhat stronger than the ventral area. The slopes in the elastic region of the central core areas were similar to the ligamentous sheath with the exception of the posterior area which was notably lower. The anterior area of the central core had the greatest yield point of the five areas, which was greater than the same area of the ligamentous sheath. The dorsal area of the central core had a substantially lower yield point than the ligamentous sheath.

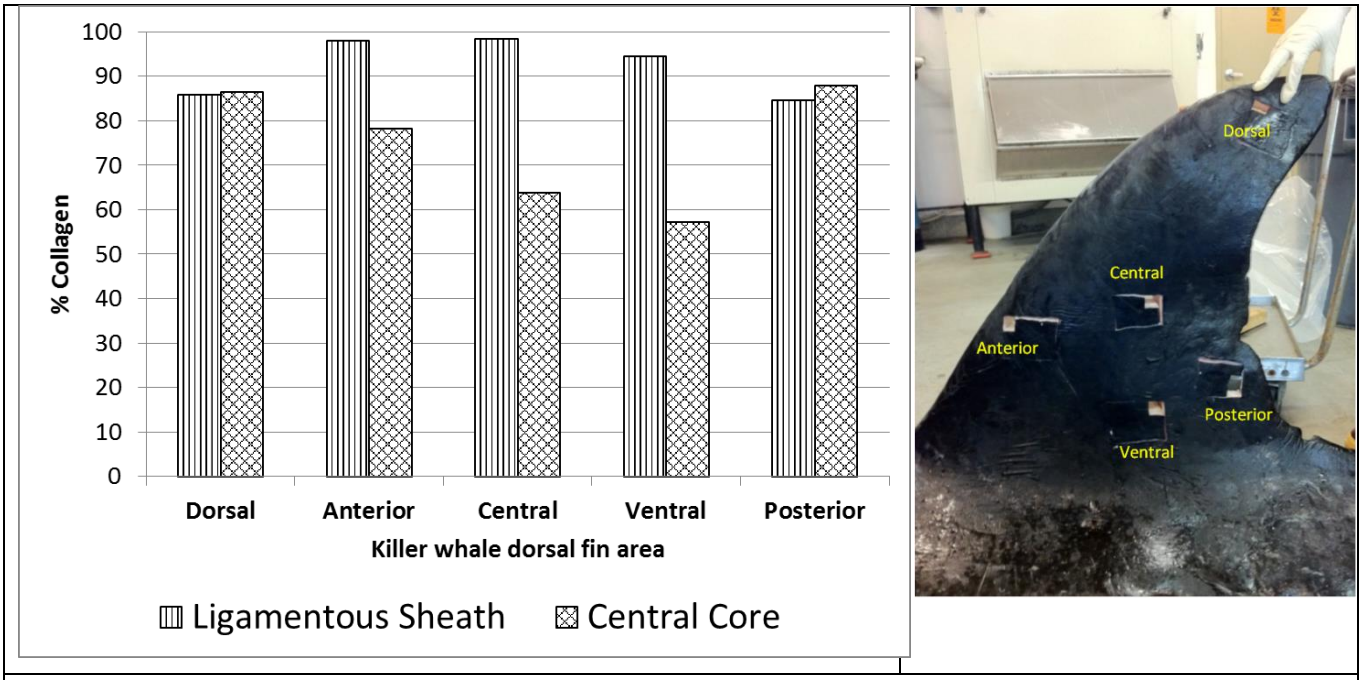

Fig. 20. Percent collagen in the ligamentous sheath and central core for five areas of the killer whale dorsal fin (shown on right).

Collagen composition - Material property comparison

Surprisingly, the material properties results did not correlate with the collagen composition values. The two species with the highest percent collagen in their ligamentous sheath, pilot whale and killer whale, had the two lowest yield points, and Blainville's beaked whale, with one of the highest yield points, had the lowest collagen percentages. A somewhat similar pattern was seen in a comparison of central core yield points and percent collagen, with the highest yield point in Blainville's beaked whale, which had the lowest percent collagen, and relatively lower yield points for pilot, false killer, and killer whale which had relatively higher percent collagen values.

The statistical analysis bears out the observed variability of the yield points when compared with percent collagen for both the ligamentous sheath and central core. For all ligamentous sheath data, there was no significant correlation between estimated yield point and percent collagen ($\rho = -0.219$, p-value = 0.574). There was a trend towards a positive correlation for the central core yield points and percent collagen ($\rho = 0.347$, p-value = 0.399), but this relationship was not significant.

Similar to the comparison between species, for the five areas tested in the killer whale dorsal fin, there was no correlation between the percent collagen and the yield point in the ligamentous sheath data ($\rho = 0.500$, p-value = 0.391), or the central core data ($\rho = 0.077$, p-value = 0.902).

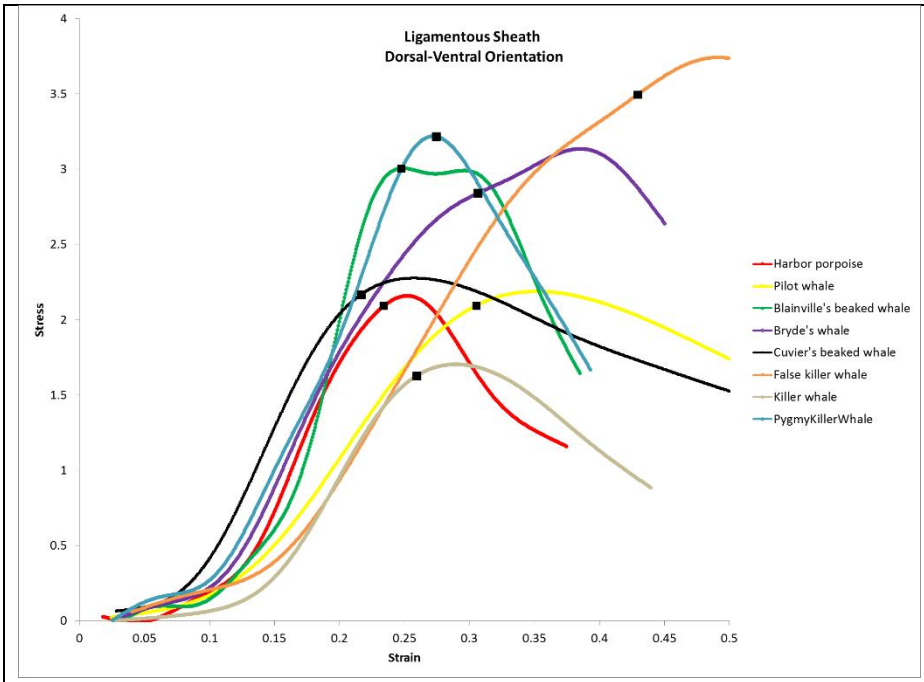

Fig. 21a. Stress/strain curves for the ligamentous sheath in the dorsal fin of eight cetacean species. Black square is estimated yield point.

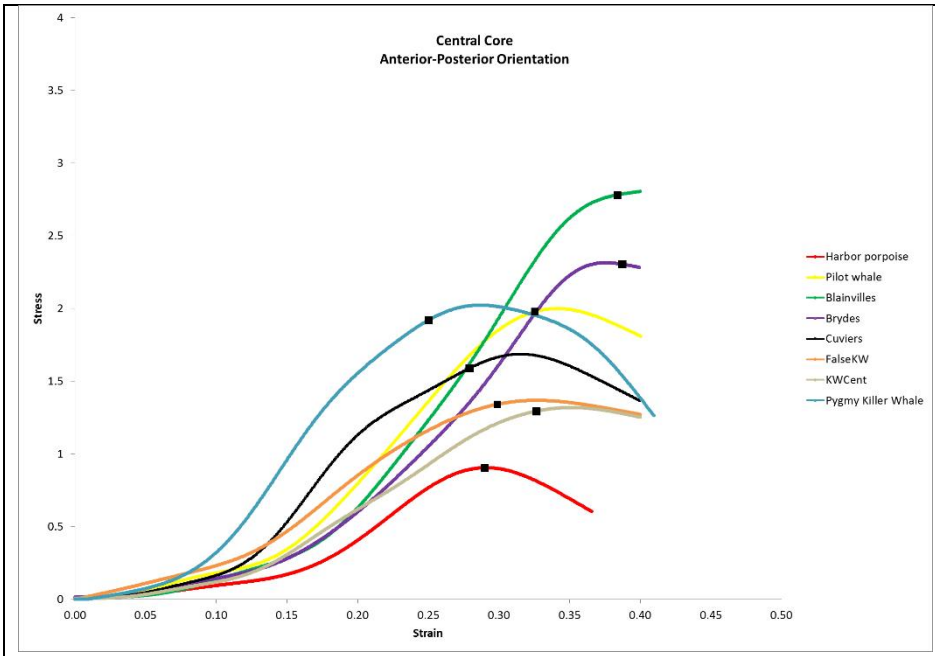

Fig. 21b. Stress/strain curves for the central core in the dorsal fin of eight cetacean species. Black square is estimated yield point.

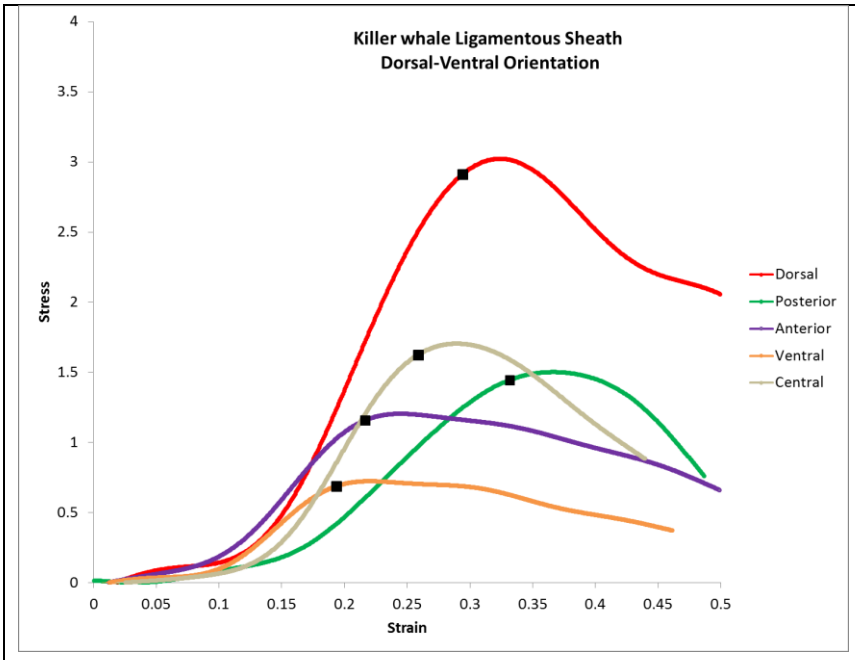

Fig. 22a. Stress/strain curves for the ligamentous sheath in five different areas of the killer whale dorsal fin. Black square is estimated yield point.

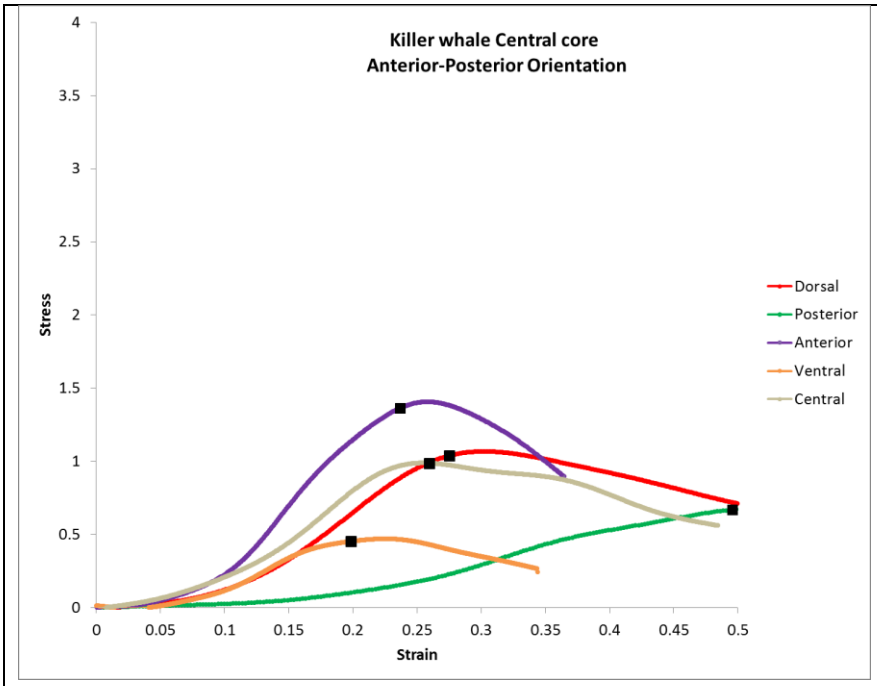

Fig. 22b. Stress/strain curves for the central core in five different areas of the killer whale dorsal fin. Black square is estimated yield point.

This study was the first to examine the material properties, and in particular the yield points, of the primary load bearing tissues in the dorsal fin of several small to medium-sized cetaceans. Therefore, comparative data are very limited, making interpretation challenging. The results of the comparison of dorsal fin tissue layers between species demonstrated that the ligamentous sheath and central core

behave like most viscoelastic tissues indicating that the testing approach was valid. In addition, the ligamentous sheath also had higher yield points and steeper slopes in the elastic region than the central core, which had lower levels of collagen, thus consistent with the expectation that greater collagen concentration would be reflected in higher strength. This trend would be expected given that the central core, on average, has a lower collagen density due to the presence of adipose cells as well as the fiber orientation being oriented in axes other than the predominate anterior-posterior (Hanson 2001). However, there was no significant relationship between the yield point and collagen content of the tissues at the species level, an unexpected outcome. While the underlying hypothesis was that tissues with more collagen would have greater strength, i.e. higher yield points, it is important to note that the strength of a tissue is not strictly a function of the collagen content, but also a function of the degree of crosslinking between the collagen fibers, a parameter that we could not directly measure. Unfortunately, none of our results for dorsal fin structure and material properties provided any strong clues regarding the large variation in tag attachment duration observed between species.

Objective #3: Performance of tags and dart attachments

WORK COMPLETED

As noted above, at the beginning of this project we discovered that the epoxy in both of the LIMPET tag models (location-only SPOT5 AM-240A-B and dive depth transmitting Mk10-A AM-266) models could potentially crack upon impact in certain cases (<3% of cases out of > 300 deployments of the SPOT5). Based on initial hydrodynamic work, we worked with engineers at Wildlife Computers to come up with alternative designs that were subsequently stressed in a variety of laboratory tests before production models were delivered to the public for whale tagging. Prototypes were thoroughly tested by repeatedly firing into a hard rubber target from 2 meters away, straight on and at an extreme angle of 45 degrees, representing a worst case scenario that should produce stresses much greater than seen in field deployments on whales. Tags were also subject to extreme testing by repeatedly striking with a 16 oz. nail hammer. All final prototypes survived these tests. A sub-sample of six depth-transmitting tags that had been impact tested and two new tags were pressurized on four repeated "dives" to 2,000m with stops every 500 meters to check for accuracy. Half of the tags were then removed from the chamber, and the other half were then run down to a maximum depth of 2,500 meters. The average error between the "true" depth and that reported by the tag at all stops was less than +/- 1%, with a maximum reported error of 1.8%. To examine resistance to longer term vibrations, we mounted an AM-240C tag on the stern bracket of a Honda 150 HP outboard. The tag was placed a few cm below the water line at rest, and during cruising this is an area that experiences high forces, both from water flowing past and impacts at the air-water interface as the stern rises and falls, along with vibrations. The boat was operated with cruising speeds around 20 knots for about 10 hours a day for 10 consecutive days. Not only did the tag survive this test, it looked almost new and most importantly the antenna and the attachment to the darts were unchanged. The new location-only model is the SPOT5AM-240C, and the new depth-transmitting model is the SPLASH10 AM-292B.

Fig. 23a. Apparatus for dart pull testing.

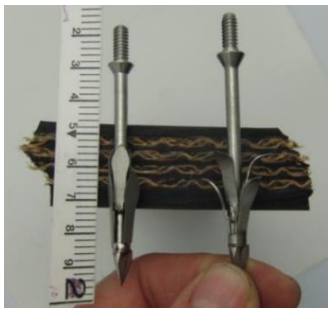

Fig. 23b. Dart testing in fiber-reinforced rubber.

Additionally we worked with Wildlife Computers on a solution that would allow our LIMPET darts to be made commercially available, with thorough testing of the new prototypes. From 2007 through mid-2012, all darts used on LIMPET tags were custom-built (model RDA-Ti). These darts were titanium Ti-6Al-4V (Grade 5) percutaneous implants with sharp tips and narrow (4 mm) shafts with two rows of backwards facing petals that permit easy insertion, even into hard dorsal fin tissue, yet result in limited wounds due to retraction occurring either due to the tissue foreign body response or interaction with conspecifics or inanimate objects (such as the seafloor). We produced the darts in two lengths, a standard dart for most species, which was 8.0 cm long, threaded at the top for insertion into the tag, such that depth of penetration was 6.7 cm. A shorter dart for smaller species was 6.0 cm long, with a penetration depth of 4.6 cm. We worked with Wildlife Computers to develop new darts (standard length model = WC-DART-007) that retained the same fundamental characteristics but that were less prone to petal breakage during dynamic loading. Darts were tested by pulling at varying loads with a custom testing apparatus (Fig. 23a) after firing single darts into simulated dorsal fin tissue (4-layer fiber-reinforced rubber, Fig. 23b) or blocks of dorsal fin tissue (Fig. 24a). Examination of how the dart elements interacted with the tissue were carried out by imaging dorsal fin tissue with implanted darts, using x-ray and MRI.

In order to assess the efficacy of the changes made to the LIMPET tags and attachment darts, and to determine what other factors might be affecting attachment durations, we reviewed the performance of SPOT5 LIMPET tags deployed on free-ranging whales. Three hundred and seven SPOT5 LIMPET satellite tags have been deployed on a total of 18 different species since 2006, as part of a collaboration between the Alaska SeaLife Center, Cascadia Research Collective and Northwest Fisheries Science Center. Detailed data were collected on each tag deployment including the version of tag, darts, and specifics about where and how the tag was attached to the whale. No two deployments are exactly the

same: angle of insertion, variation in tissue structure depending on location on the fin, individual animal behavior, variation in tissue response, etc.; any or all of these factors may play a role in attachment duration. To best assess which factors may be most important in predicting tag attachment duration, we parsed the data in several different ways, but small sample sizes often limited statistical power. Attachment durations were not normally distributed, so we used non-parametric tests and summary statistics to assess the larger dataset, and used a generalized linear model to assess a smaller subset of data from three species with the largest sample sizes.

Objective 3:

RESULTS:

The new darts now commercially available from Wildlife Computers were found to function as designed during pull tests, as demonstrated in the x-rays in Fig. 24b. The new darts were much improved in strength, resulting in an approximately 60% increase in retention strength. Additionally, their resistance to petal breakage during dynamic testing was dramatically improved.

Fig. 24a. Dart inserted into a block of pilot whale tissue and prepared for pull testing.

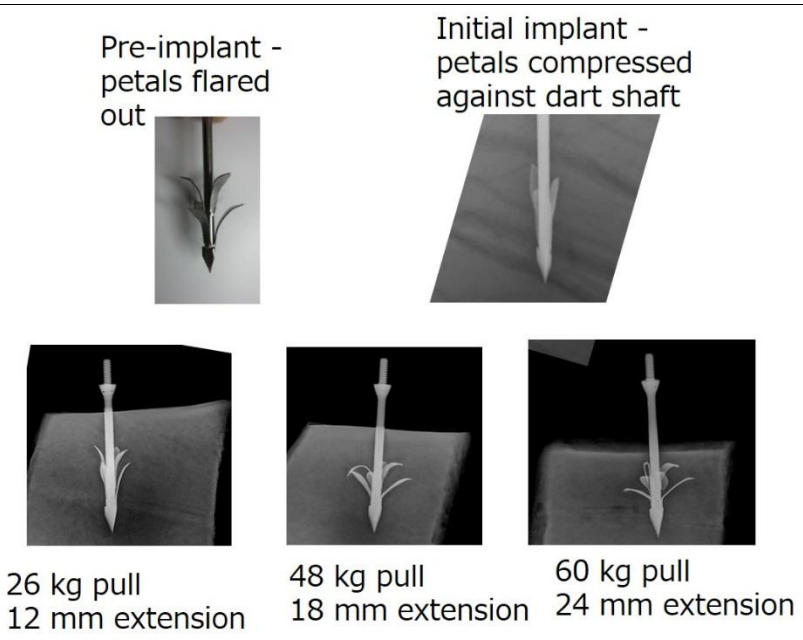

Fig. 24b. Illustration of how the petals splay out as designed during steady loading in the dart pull testing apparatus.

In our assessment of tag and dart performance, we used the metric "attachment duration", which usually reflects the time of the last Argos transmission received from the tag, because in most cases we cannot determine if transmissions ceased because tag attachment failed or the tag electronics failed. One hundred and six of the 307 LIMPET SPOT5 tagged individuals (34.5%) have been re-sighted after the last transmission from the tag, with a median time from last transmission to first sighting of 146 days (range = 1-1460). Forty-five of those individuals were photographed within 100 days of the last transmission, with photographs of 35 of sufficient quality to assess tag attachment. The tag was still attached after the last transmission in only six cases (17.1%), with a median time after last transmission of 3.5 days (range = 1-100). Based on battery voltage readings obtained prior to the cessation of transmissions, we determined that three of the six tags had stopped transmitting due to low battery

voltage, two were likely due to hardware failure of some sort, and one failure was attributed to low tag placement on the body that likely prevented any transmissions being attempted or received at the satellites. For cases where the tag was no longer attached to the fin, median sighting time after last transmission was 24 days (range = 1-99). We therefore feel that the last transmission date is most likely to correspond with the tag having been shed from the fin.

In an attempt to limit the effect of taggers with varying levels of experience and different tagging techniques, we restricted our sample to tags deployed by Cascadia Research staff, all highly trained taggers, with 91% of the tags deployed by just two individuals. The Grand median attachment duration for all SPOT5 LIMPET tag deployments, across all species, was 26.2 days, with median attachment by species ranging from a low of 4.4 to a high of 61.2 days. Tag attachment durations were highly variable, both between and within species. Fin whales were the most extreme case with a median attachment duration of 20.4 days and a range of 2.0 to 239.2 days (n = 49), with 239 days representing the longest attachment duration documented to date for a LIMPET tag.

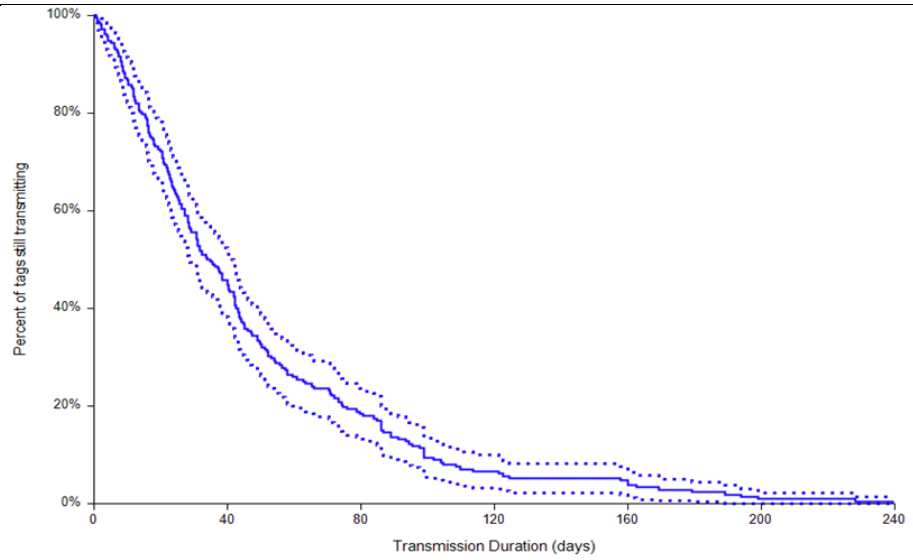

Fig. 25. Percentage of SPOT5 LIMPET tags transmitting over time, using a Kaplan-Meier estimator. Dotted lines represent the upper and lower 95th CIs. Data are from 212 SPOT5 LIMPET tags deployed on eight different species with a sample size of n>3, tagged from 2008-2014 using only standard length darts. Tags that cracked on impact and those implanted with only one dart were also excluded.

Deployments on small odontocetes and a small number of pilot whales and killer whales were conducted using shorter length darts (implantation depth of 4.6 cm). Attachment duration for short dart deployments were significantly shorter than those using standard long darts (Mann-Whitney U test, $Z = -5.9$, $p<0.00001$), so we have excluded tags with short darts from the following analyses. We further excluded tags deployed in 2006 and 2007 due to known issues with tag construction (n = 11), as well as tags documented to have cracked on impact (n = 5), tags deployed with only a single dart implanted in the fin of the tagged whale (n = 14), and species with three or fewer deployments (n= 8 tags, 4 species). Tags which never transmitted (n= 11) were also excluded. Although six tags were noted in the field to have been removed from the fin of the tagged whale during the time of observation, within days after tagging, likely due to conspecific interactions, these tags were not excluded from the analysis, as this same interaction could have occurred at any time for other deployments when observers were not there to document the removal.

The resulting dataset of 212 tags from eight species were plotted using a Kaplan-Meier Curve. Fifty percent of deployed tags were estimated to have stopped transmitting within 33.9 days of deployment, with 25% transmitting for longer than 63.5days (Fig. 25). Based on voltage readings obtained from tags prior to cessation of transmissions, 27 of the 212 tags (12.7%) likely stopped transmitting due to low battery voltage, with median attachment duration for these of 65.2 days (range = 16.0 – 199.0).

Plotted by species (Fig. 26), some interesting trends are observed: Blainville's beaked whales (n = 8) and false killer whales (n = 29) have the longest attachment duration at the point where 50% of tags have stopped transmitting. Sperm whales (n = 14) have the shortest attachment duration, at 13.5 days. However, there is a significant difference in attachment duration (two sample T-test, df = 11, T-value = -2.2342, p = 0.024) between tags deployed on sperm whales in southeast Alaska (on adult males, mean =55.8 days, n = 5) versus those deployed in Hawaii (adult females or sub-adult whales, mean = 9.4, n = 8). There are a number of factors that vary between these two samples (e.g., sex, age class, behavior), thus it is difficult to assess the source (or sources) of the difference.

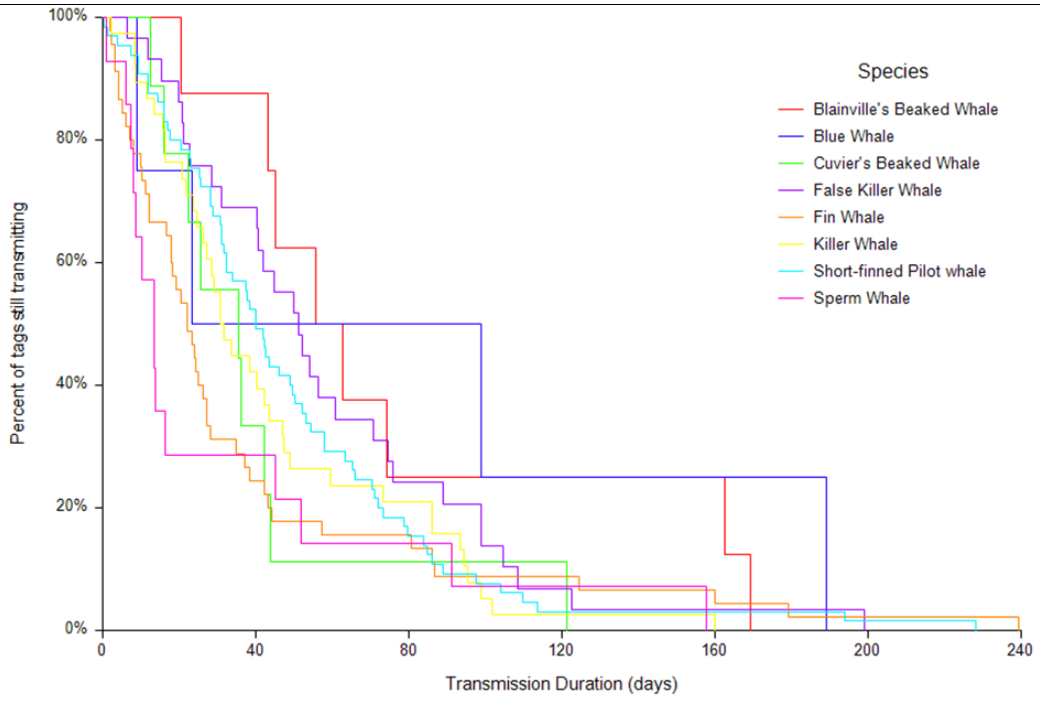

Fig. 26. Percentage of tags transmitting over time, for species with a sample of > 3 tags deployed. Same subset of data as in Fig. 25.

From 2007 until 2011, the general shape of the tag remained almost the same even though changes were made to the construction of the tag as we endeavored to make it more robust. The original tag shape is represented by all tag models of the AM-240A and B versions (Fig. 1 Left, Fig. 2). In 2011, a major change in both construction and shape of the tag occurred with the advent of the model AM-240C (Fig. 1 Right). Using the same dataset of 212 deployments described above, we compared the new tag design AM-240C (n = 82) with previous versions of AM-240A and B (n = 130). Tag models were lumped together where changes in design did not have underlying structural changes or shape changes (e.g. slightly moving the position of the wet-dry sensors) that should not have had an impact

on attachment duration. Median duration for the new tag design AM-240C was 32.0 days, compared with 36.7 d for the old tag designs, and this difference was not significant (Kruskal-Wallis One-way ANOVA, H = 2.078, df = 1, p = 0.15).

As described above, the performance of the LIMPET attachment darts were assessed using a variety of techniques, leading to several improvements over the earlier RDA-Ti dart. Use of the WC-DART-007 darts started shortly after implementation of the newest tag model (AM-S240C-1), allowing for a comparison to be made within a single tag type thereby reducing at least one possible confounding variable. There was a significant difference in attachment duration, with tags deployed using the new dart having a median attachment duration of 42.2 days (range = 0.3 – 239.2, n = 51) compared to 18.0 days (range = 2.0 – 71.0 , n = 24) for the older design (Kruskal-Wallis One-way Anova, H= 8.3, df = 1, p = 0.004). The new dart design led to a 25-195% increase in attachment duration by species with the same tag model.

To examine the effect of the tag type and remove the influence of the new dart design, we compared performance by tag model excluding deployments with the new dart (n = 57), leaving a sample of 155, then compared durations by tag model (Fig. 27). The attachment duration for the new tag model AM-240C-1 was significantly shorter than all other tag models except AM-240A-4 (Kruskal-Wallis Multiple comparison, Z-value >2.3, p <0.05). Of the 25 AM-240C-1 tags included in this analysis, 12 were fin whales with a median duration of 21 days (range = 2.0 – 57.2), so species specific differences could be contributing to this effect.

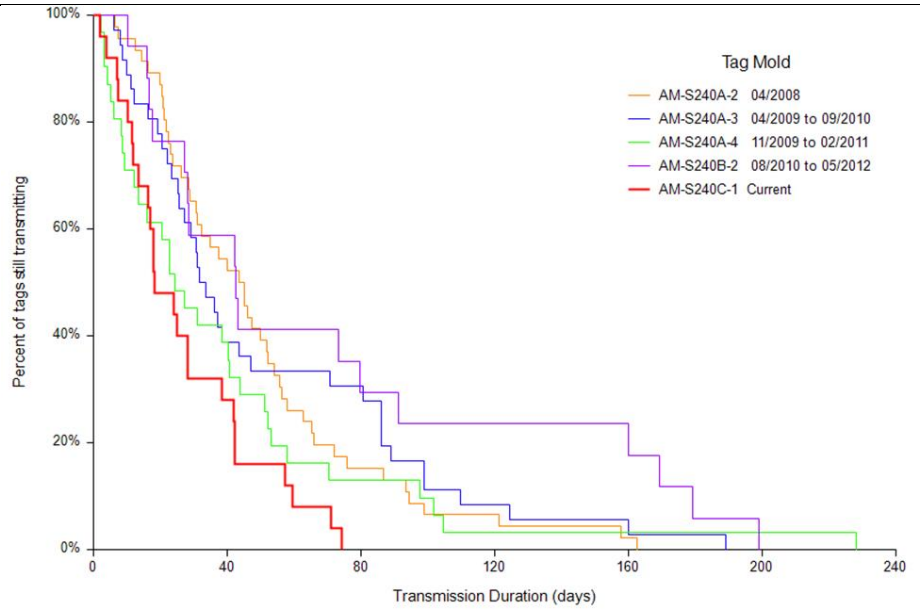

Fig. 27. Percentage of tags transmitting over time (n = 155), by LIMPET SPOT5 tag variants, excluding AM-S240C-1 tags deployed with the new dart design (WC-DART-007). Sample only includes species with a sample size of n>3, tagged from 2008-2014 using only standard length darts. Tags that cracked on impact and those implanted with only one dart were also excluded

Due to the multivariate nature of tag attachments, we utilized a generalized linear model (GLM) in R (R Core Team 2014) to assess what combination of factors might be influencing tag attachment performance. Attachment durations were not normally distributed, so we transformed the data by

taking the square root of attachment duration. In order to keep sample sizes relatively similar for each of the variables, we took a subset of data from three odontocete species with the largest number of tag deployments: short-finned pilot whales, false killer whales, and killer whales. We excluded tags documented to have cracked on impact (n = 4), tags deployed with short darts (n = 8), tags deployed with only one dart in the fin (n = 8), and tags that never transmitted. Median duration for tags deployed below the dorsal fin was considerably shorter than those in the fin (27.4 vs 37.7 days), but sample sizes were not adequate for a statistical comparison (n= 6 vs n = 126 respectively). Therefore, tags which were deployed below the dorsal fin (n = 6) were excluded, leaving 126 tag deployments. Variables assessed included vertical and horizontal placement on the fin (Fig. 28), tag model, dart model, and Angle of Attack (as described above for Objective 1). Angle of attack was assessed when photographs of the tagged animal were of sufficient quality to estimate whether the flat bottom of the tag was inclined more than ~15 degrees from the plane of the dorsal fin.

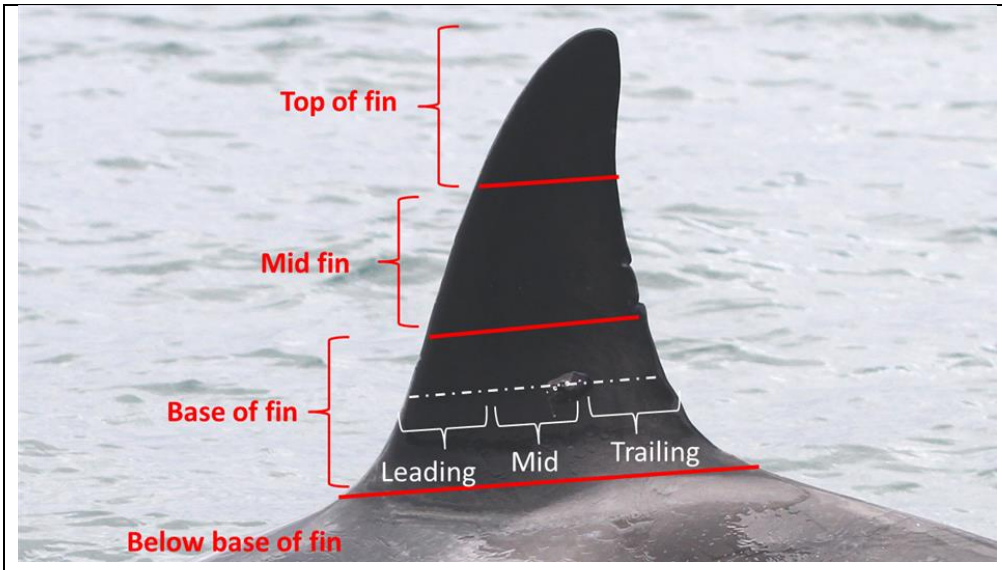

Fig. 28. Tag placement assessment. The fin is divided into three equal sections from base to top, and tag placement in one of the four vertical categories is determined. Horizontal position is either leading, mid, or trailing. If a tag overlaps two zones, tag placement is assigned to the position containing the majority of the tag. Tag pictured above had a vertical placement in the 'base" of the fin, and a horizontal placement in "mid fin". Photo by C.K. Emmons.

The overall mean attachment duration was 50.9 days (sd = 39.9, n= 126) for the subset of tags used in the GLM, and only two factors had a significant impact on attachment duration. Tags deployed with the new dart design produced by Wildlife Computers had a mean attachment duration of 54.2 days (sd = 40.3, n = 40) compared with 49.3 days (sd = 39.8, n=86) for darts of the older design. The AM-240B-2 tag model had a significantly longer attachment duration than other tag molds (mean = 67.2, sd = 63.7, n=10, compared to 49.5 days, sd = 37.2, n = 116) (Table 7). While there were trends in several other factors, none of them were significant. Notably, tags deployed with the leading edge up (into the flow of water) had a lower mean attachment duration (22.4 days, sd = 11.5, n = 13), compared to other deployments (mean = 54.2 days, sd = 40.7, n = 113), yet the results were not significant (Table 7). Mean attachment duration for killer whales (45.2 days, sd = 35.5, n=36) was shorter than both short-finned pilot whales (49.9 days, sd = 40.5, n = 64) and false killer whales (61.1 days, sd = 43.4, n = 26), but the results were not significant. Position of the tag on the fin, either vertical or horizontal, did not have an effect on attachment duration.

We also explored whether we could identify which factors might predict the unusually long attachment durations by looking at tags that lasted more than 50 days. From the sample used in the GLM analysis, false killer whales were the species with the highest proportion of tags transmitting for longer than 50 days, at 53.8%, followed by short-finned pilot whales at 39.1% and killer whales at 27.8%. All tags that had attachment durations longer than 50 days had both darts implanted into the fin, and none of them had the leading edge of the tag lifted into the flow (zero angle of attack), suggesting that these factors may be important for keeping tags attached for longer durations. We ran the GLM separately for only those tags that transmitted for > 50 days, and for this subset of tags (n = 49), the only factor that explained longer durations was the AM-240B-2 tag model.

There are clearly many variables which influence tag attachment duration, both within and among species. Remotely deployed dart tags are not surgical implants, and thus the precise angle, depth and location of tag attachment are subject to considerable variability. Individual tissue response to percutaneous darts likely also plays an important yet un-measurable role in attachment duration. In addition, substantial variation in animal behavior or other characteristics of the tagged individual are likely to play as large a role as any other single factor we can identify by looking at in-situ performance. This review of tag performance in situ does provide some important insights. While tags with a increased angle of attack in the leading edge do not have significantly shorter attachment durations despite the increased drag demonstrated by the hydrodynamics results (see Obj. 1), no tags with attachment durations over 50 days had a strong leading edge angle of attack, suggesting the increased drag and lift likely do play a role. However, the species with the longest median attachment duration, false killer whales, have a group median rate of horizontal travel more than 100% higher than fin whales, suggesting that hydrodynamic forces exerted on the tag due to increased water flow veocity likely don't play the most important role in overall attachment duration. It is possible that increased angle of attack makes the tag more susceptible to removal during contact with other whales or objects, but we have little means to test that.

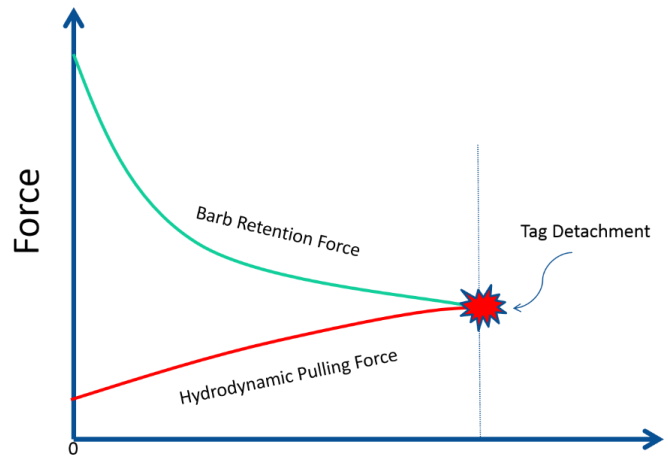

Fig. 29. Illustration of our initial view of how barb retention force of the tissue changes over time due to tissue remodeling in the wound, and how hydrodynamic pulling force was thought to increase over time as the tag migrated away from fin surface and towards the outer edge of the boundary layer. Under perfect conditions, our original hypothesis was that tag detachment occurs when this hydrodynamic pulling force exceeds the barb retention force of the tissue.

For Objective #1, we have detailed the findings from both CFD and water tunnel tests with physical models. Both methods demonstrated the previously unrecognized importance of lift in the total hydrodynamic force acting on the tag. However, the above assessment of tag performance on whales suggests one key take home message: the major factor limiting tag attachment durations is not likely static hydrodynamic force, but rather it is the sudden dynamic force of impacts with other whales or objects such as the seafloor. Our initial view of how tag detachment occurred is illustrated in Fig. 29. Although we cannot measure it directly, our visual observations of tags on whales over time and our simulations in the lab suggest that the barb retention force of the tissue decreases over time due to tissue remodeling in the wound. We originally hypothesized that the tag would eventually detach when this barb retention force was overcome by the hydrodynamic pulling force exerted on the tag, primarily by water flow. Our original hypothesis was that this hydrodynamic pulling force would increase over time as the tag migrated away from the surface of the dorsal fin and towards the outer edge of the boundary layer. However, the CFD and water tunnel testing showed that in fact the overall hydrodynamic force actually decreases at first, because as the tag starts to pull away from the fin, water flow between the tag and the fin results in less lifting force. But once the gap is more than 0.12 times the height of the tag (2.5 to 3 mm), the drag force will dominate and the total hydrodynamic force does increase as the tag pulls further away from the fin. Hence the u-shaped curve for hydrodynamic force in Fig. 30. However, our measurements of the retention force of implanted darts in carcass tissue demonstrate that this force is nearly an order of magnitude greater than the total hydrodynamic pulling force, even at very high swimming speeds. These results, along with our observations of large variability in tag attachment duration that is seemingly unrelated to any of the explanatory variables we have examined, have led us to suggest that in the vast majority of cases it is a sudden impact force that leads to tag detachment, not the slow but eventual intersection of the retention and steady hydrodynamic forces (Fig. 30).

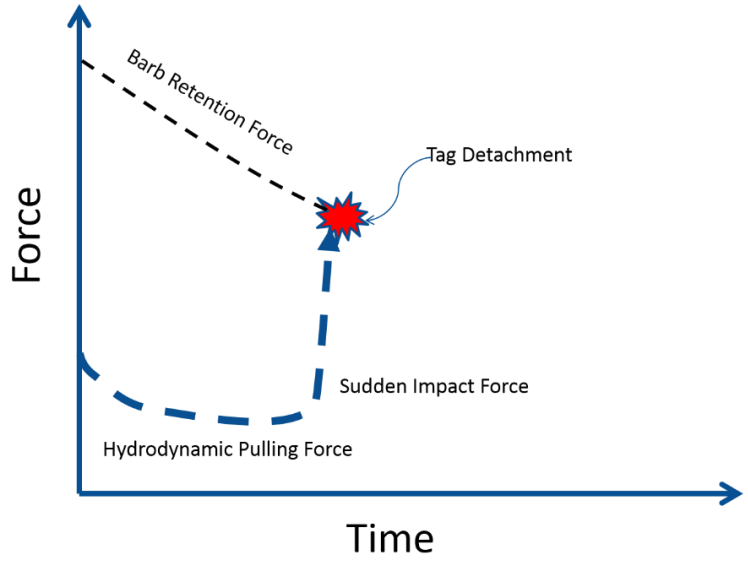

Fig. 30. Illustration of our revised view of the tag detachment process. CFD and water tunnel testing demonstrated that overall hydrodynamic force decreases at first, because as the tag starts to pull away from the fin, water flow between the tag and the fin results in less lift force. However, long before the retention force can be overcome by static hydrodynamic pulling force, most tags are likely detached by a sudden impact force that is an order of magnitude higher.

Objective #4: Tagging effects - follow-up studies

WORK COMPLETED

Assessment of the effects of tagging on survival and reproduction relied on the following approaches: 1: Obtaining follow-up photos during our own field work and from collaborators and through projects funded for other purposes. 2: Matching of photos for species that had been satellite tagged for addition to our long-term photo-ID catalogs. 3: Association analyses to identify stable groupings ("clusters") and assessments of re-sightings and reproduction of tagged individuals. 4: quantitative estimation of survival of tagged and non-tagged individuals using a capture-recapture framework, for the two species with the largest samples sizes of tags deployed and photo-identifications (false killer whales and short-finned pilot whales). This has included collection of over 300,000 photographs photographs of species that have been tagged, all oof which have been reviewed to identify tagged whales.

All photographs obtained through February 2015 of 4 of the 8 tagged species with photo-ID catalogs (false killer whales, pygmy killer whales, Cuvier's beaked whales, Blainville's beaked whales) have been matched to the catalogs to identify previously tagged individuals. Analyses of re-sighting periods are from the time of last known transmission or known tag loss (hereafter referred to as post-tag loss).

For false killer whales, the sample used for quantitative estimation of survival of tagged and non-tagged individuals included 142 distinctive and very distinctive individuals photo-identified between 2003 and 2013, with a total of 1,280 records. The dataset contained the re-sighting (capture) histories of 24 distinctive or very distinctive individuals that had been satellite tagged between 2007 and 2011. One of these had been tagged twice, for a total of 25 tag deployments. Three social clusters were identified, with tags deployed on individuals in two of the three clusters (Baird et al. 2012). For short-finned pilot whales, the photo-identification catalog contains 620 distinctive and very distinctive individuals from 34 different social clusters off Hawai'i Island between 2003 and 2012, with a total of 6,094 records. Of these, 46 individuals were satellite tagged between 2006 and 2012, in 15 different clusters containing 335 individuals. For these 15 clusters there were a total of 4,763 records. Five of these individuals were tagged twice for a total of 51 tag deployments. For both species, analyses were restricted to distinctive and very distinctive individuals with good or excellent quality photos (Baird et al. 2008; Mahaffy et al in press).

In addition to reviewing regular, visual spectrum photographs for assessment of wound healing, a forward-looking-infrared (FLIR) video camera was used to assess the relative temperature of the tag attachment site compared with the rest of the fin (Fig. 31).

Objective #4

RESULTS

The proportion of individuals re-sighted post-tag loss was relatively high even for infrequently encountered species (see Baird et al. 2013 for information on encounter rates). Pygmy killer whales have the lowest overall encounter rates of tagged insular species (Baird et al. 2013), yet five of the seven (71%) pygmy killer whales tagged prior to 2011 were re-sighted at periods from 2.81 – 5.62 years post-tag loss. Three of the tagged pygmy killer whales have been known to have had a calf born post-tag loss. Three distinctive melon-headed whales from the Kohala resident population were tagged prior to 2012, and two of the three (67%) were re-sighted post-tag loss at periods of 0.8 to 2.7 years. For Cuvier's beaked whales, eightof 10 tagged individuals were re-sighted post-tag loss at periods ranging from 0.75 to 6.9 years. Re-sighting probability for male beaked whales is lower than for females (McSweeney et al. 2007); of the four known adult females tagged, all have been re-sighted.

Two of the four re-sighted females had small calves with them when they were re-sighted at 1.5 and 1.8 years post-tag loss. Of the 10 insular Blainville's beaked whales (see Baird et al. 2011) tagged prior to 2011, seven (70%) were re-sighted post-tag loss at periods ranging from 0.01 to 5.87 years. Blainville's beaked whales have known higher dispersal rates for males than females (McSweeney et al. 2007). An assessment of the proportion of adult females re-sighted indicated 6 of 7 females from the insular population (85.7%) were re-sighted post-tag loss from 0.77- 5.87 years. Two of the six females have been sighted with calves post-tag loss.

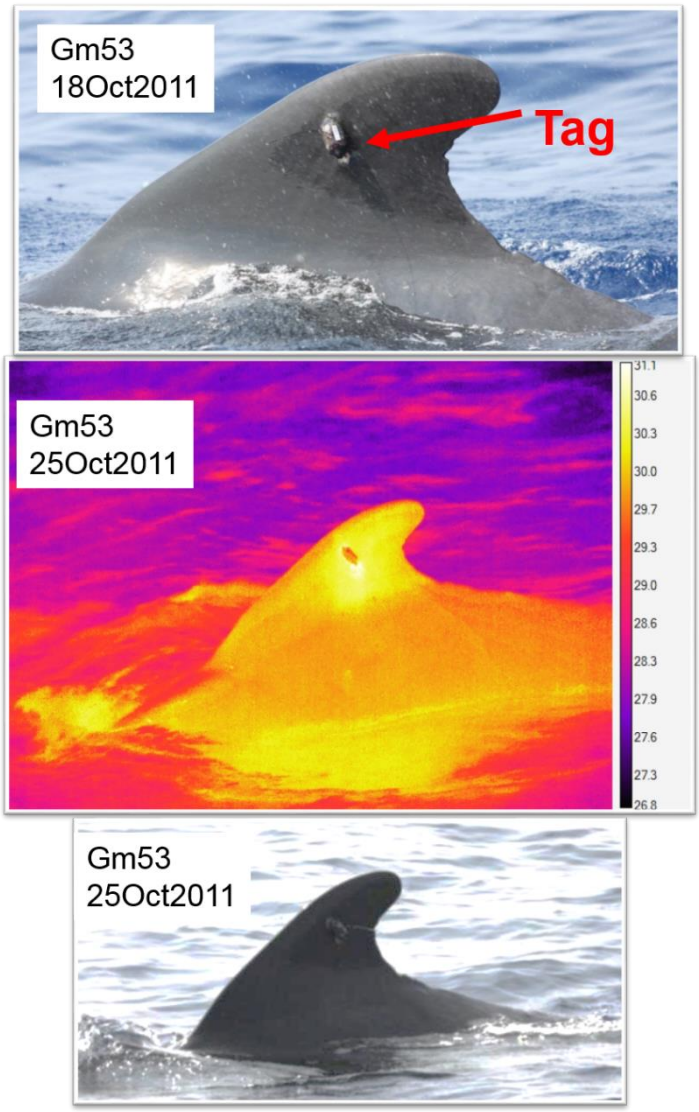

Fig. 31. Top: Photograph of short-finned pilot whale Gm53 on the day of tagging. Middle: FLIR image of Gm53 seven days after tagging. Hot colors (white) near the tag dart implant site demonstrate an increase in temperature at the implant site, and no sign of impairment of the fin's ability to dump heat. Bottom: Visual photograph taken simultaneously with the FLIR image.

Assessing reproduction of previously tagged whales of all species is limited by the relatively small number of known adult females tagged, the typically long inter-birth intervals for most species, and the long intervals between re-sighting events. For some species, e.g., melon-headed whales, no known adult females have been tagged. Besides the species noted above with calves documented post-tag loss (pygmy killer whale, Cuvier's beaked whale, Blainville's beaked whale), three of the seven known-female false killer whales that have been seen >2 years post-tag loss have been documented with calves post-tag loss. It should be noted that calving intervals for false killer whales have been estimated at seven years, and this species has a post-reproductive period later in life, thus documenting three of seven known females with calves is a relatively high rate.

Two species had sufficient sample sizes both of tags deployed and of encounters to quantitatively assess survival of tagged versus non-tagged individuals. In both cases, false killer whales and short-finned pilot whales, association analyses indicate the existence of strong, long-term association patterns with individuals grouping in "clusters" (Baird et al. 2012; Mahaffy et al. in press), so analyses considered cluster as one variable potentially influencing estimates of survival.

Modeling was conducted with R-Mark (version 2.1.5, Laake and Rexstad, 2008), an R package developed to perform estimates of demographic parameters using mark recapture techniques using the engine of software Mark. The main advantage of R-Mark is to allow the development of complex models in a more straightforward and intuitive fashion using standard formula notation in R (as opposed to having to build complex parameter index matrices – PIMS or design matrices in Mark). The analyses were conducted using the Cormack-Jolly-Seber (CJS) (Cormack, 1964; Jolly, 1965; Seber, 1965) model, which presents two main parameters: apparent survival (Phi) and capture probability (p). These parameters were modeled following the typical formulation available in Mark (White and Burnham, 1999) as well as more complex models developed by building design matrices (using R notation) for estimation of parameters as a function of covariates (e.g. a tag effect). The number of proposed models depended on the modeling approach and is specified for each of the analyses below. Model selection was performed using the Akaike Information Criterion for small samples (AICc) after accounting for overdispersion in the data (Burnham and Anderson, 2002). Overdispersion was computed using TEST1 and TEST2 in program RELEASE as a guide for goodness of fit test of a general model with full time-dependant effects (e.g. White and Burnham, 1999). Tag effects were modeled as a time-varying covariate for individuals tagged between 2007 and 2010 (false killer whales) and 2006 and 2012 (short-finned pilot whales). A single false killer whale individual tagged in 2011 was not included in the analysis because the individual was considered only slightly distinctive (Baird et al. 2008).

False killer whales: Two analyses of apparent survival were undertaken, one including all three clusters (approach 1), and one restricted to cluster 1 (approach 2), which had the majority of distinctive individuals (66), tag deployments (16 of 25), and approximately 50% (639 of 1280) records. Cluster 3, which comprised 45 individuals, had nine tag deployments and 193 records. For approach 1, 16 models were run with a combination of potential effects (Table 1). Model selection (Table 2) was performed using QAICc after accounting for overdispersion in the data (estimated c-hat = 1.87) using TEST1 and TEST2 in program RELEASE. For approach 2, restricting analyses to just Cluster 1 individuals, six models were run using a combination of effects. Model selection was performed using QAICc after accounting for overdispersion in the data (estimated c-hat = 2.37) using TEST1 and TEST2 in program RELEASE.

There is little evidence to suggest that the survival probability of tagged false killer whales is reduced relative to untagged individuals, either when modeling all clusters or only cluster 1. The best model in both cases did not show a tag effect. When all clusters are considered the point estimate of the model average survival probabilities is lower for tagged whales, but these estimates are not statistically different from non-tagged whales as indicated by the overlapping confidence intervals. Precision of the estimates of Phi for tagged whales is low likely due to the small sample of tagged whales. When all clusters are considered, capture probability for Cluster 1 individuals is relatively high (mean = 0.56), while capture probabilities for Cluster 2 (mean = 0.28) and Cluster 3 (mean = 0.27) were much lower. When only Cluster 1 is considered (approach 2), the survival estimates for tagged whales is actually slightly higher than for untagged whales, although these estimates are not statistically different, as indicated by overlapping confidence intervals.

Short-finned pilot whales: For short-finned pilot whales, two analyses were run, one taking into account all 34 social clusters (approach 1), and one restricted to the 15 social clusters that contained tagged individuals (approach 2). For the analysis considering all social clusters, cluster was not used as a covariate due to relatively small sample sizes for some clusters. A total of four models were run with a combination of effects. Model selection was performed using QAICc after accounting for overdispersion in the data (estimated c-hat = 3.17) using TEST1 and TEST2 in program RELEASE.

The results of these analyses indicated there is little evidence to suggest that the survival probability of tagged short-finned pilot whales is different from untagged individuals. In the present analysis, a tag effect was present in two of the four proposed models. The model with a tag effect ranked lower than the equivalent one without the effect. The point estimate of the model averaged Phi estimates show the survival of tagged whales being slightly higher than that of non-tagged whales, but the estimates are clearly not significantly different as indicated by their highly overlapping confidence intervals. Precision of the estimates of Phi for tagged whales is low likely due to the small sample of tagged whales. Also, the point estimates of apparent survival is relatively low (~0.9) for a long-lived cetacean such as short-finned pilot whales. The low values are biased because some of the clusters sampled in this study have not been seen frequently. If animals are alive but not often detected, the model interprets them as "dead" and the estimated survival parameter is underestimated. The approach below attempt to deal with this issue by selecting the subset of the short-finned pilot whale clusters that included tagged individuals

For the analysis including only those 15 clusters that included tagged individuals, it was possible to include cluster as a covariate as the number of capture events per cluster was greater. For this analysis a total of 16 models were run with a combination of the effects. Model selection was performed using QAICc after accounting for overdispersion in the data (estimated c-hat = 3.70) using TEST1 and TEST2 in program RELEASE. The survival estimates (~0.96) obtained with approach 2 are more consistent with a long-lived marine mammal such as short-finned pilot whales and therefore are preferred relatively to approach 1. Once again, there is little evidence to suggest that the survival probability of tagged whales is different from untagged individuals. Models with tag effect ranked lower than their equivalent model without this effect. For example, the best model provides a better fit than the equivalent model with a Tag effect. The predicted survival probability for a tagged whale is nearly the same as that of an untagged individual and is clearly not statistically different. Wide confidence intervals of Phi for tagged whales are a result of a relatively small sample size.

Power to detect tag effects: One of the main questions in estimating survival of tagged and non-tagged whales relates to the power of the statistical models to detect the tag effect. In general, cetacean

satellite tagging studies have small sample sizes primarily because of the relatively high cost of the instruments. The power to detect a tag effect in capture-recapture studies such as those described above depends on the magnitude of the effect, whether the effect is acute or chronic, the sample sizes (e.g. number of capture occasions, proportion of the population tagged), the capture probability, and the precision of the parameter estimates. One way to assess the power to detect a tag effect for capture-recapture studies is through simulation. Estimates of model parameters such as those provided above can be used to simulate a population under circumstances that match the sampling scheme of the study in order to assess the probability a tag effect is correctly estimated given the parameters and the model structure.

Preliminary simulations assuming a yearly survival estimate of 0.95 for both false killer and short-finned pilot whales and that 2.5% of the population is tagged every year for a period of 10 years were conducted using average values of capture probability consistent with those reported above ($p=0.4$ for false killer whales and $p=0.7$ for short-finned pilot whales). These simulations show that high probabilities to detect a tag effect require significantly large tag effects. In the example provided above, mortality has to increase from 5% per year to 17.5% - 25% per year for the probability of detecting the effect to exceed 75%.

These simulations must be considered preliminary because other potential factors that influence the precision of the model parameter estimates (and therefore the ability to detect an effect) are not considered. For example, the simulation assumes that the capture-recapture model is known, when in reality model uncertainty is incorporated in the estimation process (e.g., via model selection procedures). In addition, there was no variability added to the parameters of the simulation model. For example, capture probability and the proportion of tagged animals is constant across capture occasions. Adding variability would likely increase variance estimates of the model parameters and decrease power. Despite that, the simulations provide evidence that the power to detect a tag effect is small in tagging studies of false killer and short-finned pilot whales in Hawai‘i because the tag effect for LIMPET tags is likely negligible, and because the number of tags deployed is low and variable across years.

FLIR thermal imaging of tagged whales confirmed that LIMPET tagging did not compromise the ability of the fin vasculature to radiate heat. The area of the tag implant site was always warmer or the same temperature as the rest of the dorsal fin. There was no sign of a disruption of the vasculature in a way that could significatly compromise the function of the dorsal fin to act in its thermoregulatory role. Evaluation of post-tagging photographs for assessment of wound healing is ongoing, but we can conclude that in the cases where the LIMPET tag was successfully deployed with no cracking of tag or dart components, the tag was eventually shed by outward migration of the darts from the dart entry holes, with the exception of two Blainville's beaked whales where posterior migration of darts may have occurred. The wound healing process appears to proceed through normal stages, with tissue proliferation and remodeling typically occurring within three months. Remodeling and repigmentation was usually complete within one year, although in some cases limited scarring, with small, persistent depigmented areas or small (<2 cm diam., < 1 cm height) depressions or swellings. We observed no signs of infection.

We have no evidence to suggest that the LIMPET tagging technique has any significant adverse long-term impacts on health or survival, and accumulating evidence from observations of calving by several species of previously tagged whales, including one that turned out to have been pregnant during tag attachment, suggest no significant impact on reproduction. While our overall results are being

integrated into improved LIMPET tag and attachment designs, we feel it is appropriate to recommend the current system for medium-sized cetaceans, even those that are endangered.

IMPACT/APPLICATIONS

Understanding the potential for impacts of naval activities on protected species of marine mammals and mitigating such impacts requires information on movements and habitat use. The development of better tag technologies and deployment techniques will make a significant contribution to the ability of researchers to track movements, monitor behavior, and determine distribution of species of interest.

TRANSITIONS

The improved versions of the LIMPET satellite tag and attachment system that were developed during this project are now commercially available from Wildlife Computers (Seattle, WA), and LIMPET tags are being acquired by and deployed by multiple organizations (e.g. Southwest Fisheries Science Center, Cascadia Research Collective, Woods Hole Oceanographic Institution, among many others) in other projects funded by the US Navy to monitor marine mammals on Navy ranges and elsewhere.

RELATED PROJECTS

The National Marine Fisheries Service Pacific Islands Fisheries Science Center is supporting research on false killer whale movements in Hawaiian waters (Baird et al. 2010; 2012), and the Naval Postgraduate School (with funding from N45), the Living Marine Resources Porgram and Commander, Pacific Fleet have supported tagging studies of a variety of species in various locations. Tag and deployment developments from this work are being incorporated into these ongoing studies. For example, see: www.cascadiaresearch.org/hawaii/beakedwhales.htm
www.cascadiaresearch.org/hawaii/falsekillerwhale.htm
www.cascadiaresearch.org/SCORE/SCOREMain.htm
A project to develop a LIMPET tag including FastlocGPS capability for more precise and frequent position estimates commenced in 2014, in collaboration with David Moretti, Naval Undersea Warfare Center, Newport, RI, funded by the DoD Environmental Security Technology Certification Program.

ACKNOWLEDGMENTS

Valuable assistance and collaboration was provided by many, including Roger Hill, Melinda Braun, Todd Lindstrom, Matthew Rutishauser, Shawn Wilton, Andy Leask and other staff at Wildlife Computers; Daniel McSweeney of Wild Whale Research Foundation; Dr. Stephen Raverty of the Animal Health Center, B.C. Ministry of Agriculture and Lands; Frank Fish of West Chester University; Alex Zerbini, Daniel Webster, Sabre Mahaffy, Jessie Huggins and Jessica Aschettino of Cascadia Research Collective; Julianna Houghton, Eric Ward, Mark Myers, Mary Jean Willis, and Tom Lee of Northwest Fisheries Science Center; Kobi Johnson of the Animal Emergency Center and Puget Sound Veterinary Referral Center; Kristi West of Hawaii Pacific University; and Sue Herring and Tracy Popowics, University of Washington. Thanks to Deron Verbeck, Stacia Goecke, Julian Tyne, Tori Cullins, Jim Ward, and Alicia Franco for providing follow-up photographs. Research on cetaceans in Hawaii was approved by the Institutional Animal Care and Use Committees of Alaska SeaLfe Center and Cascadia Research and authorized by NOAA Fisheries Marine Mammal Research Permits 731-1774 and 15330.

REFERENCES

Andrews, R.D., Baird, R.W., and G.S. Schorr. 2010. Development of improved attachment systems and techniques for monitoring beaked whales. Final Report ONR Grant Number N000140811203. 12p. Alaska SeaLife Center, Seward, AK. Supported by the Office of Naval Research.

Baird, R.W., G.S. Schorr, D.L. Webster, D.J. McSweeney, M.B. Hanson, and R.D. Andrews. 2010. Movements and habitat use of satellite-tagged false killer whales around the main Hawaiian Islands. Endangered Species Research 10:107-121.

Baird, R.W., M.B. Hanson, G.S. Schorr, D.L. Webster, D.J. McSweeney, A.M. Gorgone, S.D. Mahaffy, D. Holzer, E.M. Oleson and R.D. Andrews. 2012. Range and primary habitats of Hawaiian insular false killer whales: informing determination of critical habitat. Endangered Species Research 18:47-61

Baird, R.W., A.M. Gorgone, D.J. McSweeney, D.L. Webster, D.R. Salden, M.H. Deakos, A.D. Ligon, G.S. Schorr, J. Barlow and S.D. Mahaffy. 2008. False killer whales (*Pseudorca crassidens*) around the main Hawaiian Islands: long-term site fidelity, inter-island movements, and association patterns. Marine Mammal Science 24:591-612.

Baird, R.W., G.S. Schorr, D.L. Webster, D.J. McSweeney, M.B. Hanson, and R.D. Andrews. 2010. Movements and habitat use of satellite-tagged false killer whales around the main Hawaiian Islands. Endangered Species Research 10:107-121.

Baird, R.W., G.S. Schorr, D.L. Webster, S.D. Mahaffy, D.J. McSweeney, M.B. Hanson, and R.D. Andrews. 2011. Open-ocean movements of a satellite-tagged Blainville's beaked whale (*Mesoplodon densirostris*): evidence for an offshore population in Hawai‘i? Aquatic Mammals 37:506-511.

Baird, R.W., M.B. Hanson, G.S. Schorr, D.L. Webster, D.J. McSweeney, A.M. Gorgone, S.D. Mahaffy, D. Holzer, E.M. Oleson and R.D. Andrews. 2012. Range and primary habitats of Hawaiian insular false killer whales: informing determination of critical habitat. Endangered Species Research 18:47-61

Baird, R.W., D.L. Webster, J.M. Aschettino, G.S. Schorr and D.J. McSweeney. 2013. Odontocete cetaceans around the main Hawaiian Islands: habitat use and relative abundance from small-boat sighting surveys. Aquatic Mammals 39:253-269.

Burnham, K.P. and Anderson, D.R. (2002). Model Selection and Multimodel Inference: a Practical Information-theoretic Approach. 2nd ed. Springer- Verlag, New York. 488pp.

Cormack, R. M. (1964). Estimates of survival from the sighting of marked animals. Biometrika 51, 429–438.

Hanson, M.B. 2001. An evaluation of the relationship between small cetacean tag design and attachment durations: a bioengineering approach. Ph.D. dissertation, Univ. of Washington, Seattle, WA. 208 pp.

Jolly, G. M. (1965). Explicit estimates from capture–recapture data with both death and immigration stochastic model. Biometrika 52, 225–247

Laake, J. and Rexstad, E.A. (2008). RMark – an alternative approach to building linear models in MARK. In: Cooch, E. and White, G.C. (eds). Program MARK: a gentle introduction. 690pp. [Available at: http://www.phidot.org/software/mark/docs.book].

Mahaffy, S.D., R.W. Baird, D.J. McSweeney, D.L. Webster and G.S. Schorr. In press. High site fidelity, strong associations and long-term bonds: short-finned pilot whales off the island of Hawai‘i. Marine Mammal Science.

Mittal, R., H. Dong, M. Bozkurttas, F.M. Najjar, A. Vargas, and A. von Loebbecke. 2008. A versatile sharp interface immersed boundary method for incompressible flows with complex boundaries. J. of Computational Physics 227: 4825-4852.

McSweeney, D.J., R.W. Baird and S.D. Mahaffy. 2007. Site fidelity, associations and movements of Cuvier's (*Ziphius cavirostris*) and Blainville's (*Mesoplodon densirostris*) beaked whales off the island of Hawai‘i. Marine Mammal Science 23:666-687.

Seber, G. A. F. (1965). A note on the multiple recapture census. Biometrika 52, 249–259.

Schultz, M.P., and K.A. Flack. 2003. Turbulent boundary layers over surfaces smoothed by sanding. J. Fluid Engineering 125:863-870.

Weber, P.W., L.E. Howle, M.M. Murray and F.E. Fish. 2009. Lift and drag performance of odontocete cetacean flippers. J Exp Biol, 2009. 212: 2149-2158.

Weber, P.W., L.E. Howle, and M.M. Murray. 2010. Lift, drag, and cavitation onset on rudders with leading-edge tubercles. Marine Tech SNAME News. 47(1): p. 27-36.

White, G.C. and Burnham, K.P. (1999). Program MARK: Survival estimation from populations of marked animals. Bird Study 46 (Supplement): 120– 38.

PUBLICATIONS and PRESENTATIONS

Andrews, R.D., Baird, R., Hanson, B.M., Howle, L., Mittal, R., Schorr, G., and Wilton, S. 2014. Improving attachments of remotely-deployed dorsal fin-mounted tags: tissue structure, hydrodynamics, in situ performance, and tagged-animal follow-up. *In:* Abstracts of the 5th International Bio-Logging Science Symposium, Strasbourg, France, September 22-27, 2014. [oral conference presentation].

Andrews, R.D., Baird, R., Webster, D., Wilton, S., Lindstrom, T. 2014. The Whale Lander and SpicyTalk – A solution for recording high-resolution behavior from cetaceans for days to weeks with recoverable, archival transmitting tag. *In:* Abstracts of the 5th International Bio-Logging Science Symposium, Strasbourg, France, September 22-27, 2014. [poster conference presentation].

Andrews, R.D., Quakenbush, L.T., Goertz, C.E.C., and Hobbs, R.C. 2014. LIMPET tag as an alternative method for satellite tagging beluga whales. *In:* Abstracts of the Cook Inlet Beluga Whale Conference, April 5, 2014. Anchorage, AK. [oral conference presentation].

Barlow, J., Tyack, P.L., Johnson, M.P., Baird, R.W., Schorr, G.S., Andrews, R.D., and Aguilar de Soto, N. (2013). Trackline and point detection probabilities for acoustic surveys of Cuvier's and Blainville's beaked whales. Journal of the Acoustical Society of America 134(3):2486–2496. [published, refereed].

Ford, J.K.B., Durban, J.W., Ellis, G.M. Towers, J.R., Pilkington, J.F., Barrett-Lennard, L.G., and Andrews, R.D. (2013). New insights into the northward migration route of gray whales between Vancouver Island, British Columbia, and southeastern Alaska. Marine Mammal Science 29(2): 325–337. [published, refereed].

Mathias, D., Thode, A.M., Straley, J., and Andrews, R.D. (2013). Acoustic tracking of sperm whales in the Gulf of Alaska using a two-element vertical array and tags. Journal of the Acoustical Society of America 134(3):2446-2461. [published, refereed].

Moore M., Andrews, R., Austin, T., Bailey, J., Costidis, A., George, C., Jackson, K., Pitchford, T., Landry, S., Ligon, A., McLellan, W., Morin, D., Smith, J., Rotstein, D., Rowles, T., Slay, C., and Walsh, M. (2013). Rope trauma, sedation, disentanglement, and monitoring-tag associated lesions in a terminally entangled North Atlantic right whale (*Eubalaena glacialis*). Marine Mammal Science 29(2):E98–E113. [published, refereed].

Reisinger, R.R., Oosthuizen, W.C., Péron, G., Cory Toussaint, D., Andrews, R.D., de Bruyn, P.J.N. (2014) Satellite tagging and biopsy sampling of killer whales at subantarctic Marion Island: effectiveness, immediate reactions and long-term responses. PLoS ONE 9(11): e111835. [published, refereed].

Schorr, G.S., Falcone, E.A., Moretti, D.J., and Andrews, R.D. (2014). First long-term behavioral records from Cuvier's beaked whales (*Ziphius cavirostris*) reveal record-breaking dives. PLoS One 9(3): e92633. [published, refereed].

Straley, J.M., Schorr, G.S., Thode, A.M., Calambokidis, J., Lunsford, C.R., Chenoweth, E.M., O'Connell, V.M., and Andrews, R.D. (2014). Depredating sperm whales in the Gulf of Alaska: local habitat use and long distance movements across putative population boundaries. Endangered Species Research 24:125-135. [published, refereed].